CR 86213

FINAL REPORT

DESIGN CRITERIA FOR RADAR TRACKING SYSTEMS

By Howard C. Salwen and David M. Warren

19 April 1968

Prepared under Purchase Order #ER-13,784

National Aeronautics and Space Administration
Electronics Research Center
Cambridge, Massachusetts

ADVANCED COMMUNICATIONS INFORMATION MANAGEMENT

RESEARCH • DEVELOPMENT • ENGINEERING

ADCOM

A TELEDYNE COMPANY

Mr. Janis Bebris
Technical Monitor
575 Technology Square
Cambridge, Massachusetts 02139

Requests for copies of this report should be referred to:

National Aeronautics and Space Administration
Electronics Research Center
Cambridge, Massachusetts 02139

FINAL REPORT

DESIGN CRITERIA FOR RADAR TRACKING SYSTEMS

By Howard C. Salwen and David M. Warren

19 April 1968

Prepared under Purchase Order # ER-13,784
ADCOM
A Teledyne Company
808 Memorial Drive
Cambridge, Massachusetts 02139

National Aeronautics and Space Administration
Electronics Research Center
Cambridge, Massachusetts 02139

TABLE OF CONTENTS

TABLE OF CONTENTS (Cont.)

LIST OF ILLUSTRATIONS

LIST OF ILLUSTRATIONS (Cont.)

FINAL TECHNICAL REPORT
DESIGN CRITERIA FOR RADAR TRACKING SYSTEMS

By Howard C. Salwen and David M. Warren

ADCOM, A Teledyne Company
Cambridge, Massachusetts

SUMMARY

This report reviews the theoretical aspects of the radar tracking problem. Derivations are given to show the importance of matched filters, ambiguity diagrams and maximum likelihood detectors to radar system design.

The practical aspects of radar system design are discussed. In particular, the precision obtainable from phase-locked loops, split gate trackers, leading edge trackers and harmonic range tone trackers are derived in terms of their design parameters and performance requirements.

GENERAL INTRODUCTION

This document constitutes the Final Technical Report prepared by ADCOM, a Teledyne Company, for NASA Electronic Research Center, Cambridge, Massachusetts under Purchase Order No. ER-13, 784.

The object of the study program is to outline several important results of radar theory and to relate these results to practical tracking implementations. In particular, the accuracy limitation of several accepted tracking techniques are derived and discussed in terms of their application to laser altimetry and range finding.

The contents of the report are as follows: An extensive review of the theoretical aspects of the radar tracking problem is presented. This review treats the utility of matched filter detection, the importance of ambiguity functions to radar signal design, and shows theoretical accuracies achievable with maximum likelihood detection. The theoretical discussion is followed by a presentation of the performances practically achievable with phase-locked loops, split gate and leading edge range tracking systems, and harmonic range tone systems. Three appendices are included which contain detailed derivations of several theoretical results, and detailed derivations of the noise and dynamic performances of the four practical techniques mentioned above.

SUMMARY OF DESIGN CRITERIA FOR RADAR TRACKING SYSTEMS

Introduction

This section presents background summary material on the operation of radar tracking systems. There are a variety of such systems and a number are available commercially. Each has distinguishing features of operation which recommend its use for specific situations. An analysis of these systems is desirable to serve as a guide in the selection of the appropriate system for a given tracking situation. Fortunately, the variety of systems can be characterized in terms of a few simple models whose operation is governed by the same theoretical considerations. It is, therefore, possible to compare these systems in terms of the same theory of operation so that the features of each system are readily discerned.

Types of Systems Considered

Four basic types of tracking systems are considered here. They are:

1) Phase-Locked Loop
2) Split Gate Range Tracker
3) Leading Edge Range Tracker
4) Harmonic Tone Ranging System

The phase-locked loop is used to track a sinusoidal signal waveform such as the carrier of a radar signal. In general, it is used with a CW signal rather than a pulsed signal so that its primary use is found with CW radar and telemetry where the carrier and possibly a number of subcarriers are always present. In its operation it is able to sense the phase of the input signal and provide an output sinusoid whose phase is an accurate duplicate of the input phase. When the input signal is composed of a

number of subcarriers, or is modulated with a set of ranging tones, the phase-locked loop is used as a coherent demodulator to extract the desired subcarriers or range tones.

The split gate range tracker is used to track a pulse radar signal. It tracks a periodic pulse signal and is designed to operate with a specific signal pulsewidth. It may be used in an altimeter, though it must be borne in mind that in a practical situation , such as altimetry, there may be a number of echos received almost simultaneously from terrain of similar altitudes. In practice, these echo pulses may overlap each other resulting in an altitude error since the split gate tracker characteristically tracks the center of gravity of the returned pulses. The split gate range tracker also functions as a filter to smooth out or reduce the effects of noise on the input signal. Thus its output signal is, ideally, a smooth periodic pulse train, synchronized with the input, yet unperturbed by the input noise.

The leading edge range tracker is similar to the split gate range tracker. The basic difference is in the method of sensing the time of occurrence of the input pulse. While the split gate range tracker senses the center of gravity of the pulse, the leading edge range tracker senses a point on the leading edge of the pulse. Otherwise, the two systems are the same. The major advantage of the leading edge tracker is found in the situation where a number of echo pulses arrive at approximately the same time with possible overlapping of the pulses. The leading edge of the first pulse of the group of pulses is the range which is measured. The remaining pulses have little or no effect on the range measurement. This is a distinct improvement over the performance of the split gate tracker described above in the altimetry application.

The harmonic tone ranging system operates with a specially generated signal composed of several ranging tones modulated onto a carrier. In radar ranging applications, this signal may be reflected off the target or retransmitted via a transponder. An important advantage of this system is found in those situations where a transponder is required since the sinusoidal type of signal can be reproduced by a transponder to a much higher degree of precision than a pulse type signal. Also, this system can handle higher data rates in those situations where a pulse system would be limited by the pulse repetition frequency. This system also enjoys the advantage of a signal design which most closely approximates the theoretical limit of precision, that is, a signal whose important spectral lines are placed at the outer edges of the allowable signal bandwidth. The system measures range by comparing the phases of the received ranging tones against a set of reference tones. This form of measurement has inherent range ambiguities which can be resolved by arithmetic operations on the phase measurements of the various tones.

In practice the phase-locked loop is frequently included as one of the components of a harmonic tone range tracker. A set of these are well suited for extracting the ranging tones and, in addition, it is possible to utilize the data provided by the carrier tracking loop to derive increased precision from the tone tracking loops. In this respect the phase-locked loop is not regarded as a competitor of the harmonic tone range tracker but as an integral part of that technique.

The question of which system to use in a given application depends on a number of factors which include the available power, the type of signal source, i. e., pulse or CW, and the nature of the signal transmission channel. A discussion of all these factors is beyond the scope of this report, but it should be mentioned that the latter factor includes such considerations as the nature of the terrain which is particularly important

in alimetry. Its importance is due to the presence of multiple echos which are found particularly in mountainous regions. The performance of each of the systems considered is affected by the presence of multiply reflected signals, so that this represents an important consideration in the final selection of the system.

Fundamental Theory

The underlying theory which defines and limits the range measurements is common to all of the systems. The reason for this becomes apparent when certain aspects of the measurement procedure are examined.

In each case a measurement is made of the signal in the presence of some noise background. Noise is always present whether it is generated in the receiver itself or comes from outer space. Irrespective of the type of measurement which is made or of the particular system considered, the theory relating to the measurement of signal in the presence of noise is controlling.

In each case the input to the tracking device is a signal of limited bandwidth. The limitation is imposed by either the transmitter or the receiver characteristics. In any event, the important point here is that filtered signals are being processed so that filter theory applies to each system. The same applies also to the signal processing techniques since each system can be characterized by a filter with respect to both the dynamic and noise responses.

The question may be raised as to whether the fact that one system utilizes pulses while the other is CW results in a significant difference in their measurement capability. The answer is given by the well-known sampling theory which shows that the measurement is equally good whether the input data is observed continuously or whether it is observed in the

form of pulses so long as the pulse repetition frequency is above the required output data rate. The only difference between the two basic techniques is related to the degree of complexity required to achieve the theoretically predicted performance in each case.

The theory is basic to radar ranging techniques in which the time of signal propagation over the unknown distance is measured. The results of the theory are equally applicable to signals transmitted at the low and high frequency portions of the electromagnetic spectrum because the signals are described in terms of their baseband representations. The results are directly applicable to laser ranging devices under conditions of gaussian noise. The theoretical aspects of the radar problem are presented in detail in Appendix A.

The classical radar problem is concerned with the task of obtaining the best ranging accuracy for a given signal waveform in the presence of gaussian noise. The optimum accuracy is obtained when the receiver filtering has the correct relationship to the signal spectrum. More specifically, the task is to determine the specific form of the receiver filter weighting function h(t) which maximizes the signal-to-noise ratio at the output of the filters at a given sampling time $t = T$.

The solution to this optimization problem for the case of additive white gaussian noise is well known. The optimum linear system, H(s), is a matched filter, sometimes called a correlation detector. This solution has wide application since, in most cases, receiver input noise can be reasonably described as white gaussian.* Simply stated, the impulse response of the optimum linear system is the mirror image of the input waveform, shifted by the time duration T of the signal, that is,

*Note that given enough smoothing, poisson noise takes on a gaussian characteristic.

$h(\tau - t) = s_i(t)$ where $s_i(t)$ is the input signal. The output signal of the filter is given by

$$S_o(\tau) = \int_0^{\tau} s_i(t)\, h(\tau - t)\, dt \qquad (1)$$

for any $h(t)$ and yields the highest SNR when $h(\tau - t) = s_i(t)$.

The presence or absence of a target-returned signal is determined by subsequent operations on the filter output $y(t) = s_o(t) + n_o(t)$ which is the sum of the output signal $s_o(t)$ and the output noise $n_o(t)$. If $y(t)$ is above a threshold y_o it is decided that a target is present, below y_o it is decided that there is no target. The exact level of the threshold is fixed by trading off the probability of detection of a target in a noisy environment against the probability of false alarm. As the threshold is raised it becomes less likely that the noise alone will exceed the threshold and cause a false alarm. At the same time, it becomes less likely that the signal and noise will exceed the threshold when a target is present. Graphs of probability of detection versus probability of false alarm show that the probability of detection is high and that of false alarm is low with good signal-to-noise ratios. Less favorable results are obtained with poor signal-to-noise ratios or with a fluctuating signal amplitude such as a Rayleigh distributed signal amplitude.

Another useful concept in signal analysis is the ambiguity diagram which is a three-dimensional plot of the signal's ambiguity function. This function is the magnitude of correlation of the complex envelope $\mu(t)$ of the input signal, $s_i(t)$, with the doppler shifted complex envelope. That is,

$$\chi(\tau, \omega) = \left| \int_{-\infty}^{\infty} \mu(t)\, \mu^*(t + \tau)\, e^{j\omega t}\, dt \right| \qquad (2)$$

A convenient representation in two dimensions is the 3 dB contour of the ambiguity function.

This diagram provides a great deal of information about the utility of a specific signal design. For example, in the case of a periodic pulse train consisting of several pulses, the two-dimensional diagram takes the form of a set of ellipses in both the time and frequency dimensions. By way of contrast, if a single signal pulse is transmitted, the diagram consists of only one ellipse at the origin of the coordinates. The reason for the name is now apparent for, in the case of a periodic pulse signal, the spacing of ellipses along the time axis represents the "once around again" range ambiguities, while the spacing along the frequency axis represents the doppler ambiguities caused by the line spectrum of the signal. In practice, doppler ambiguities may be noticed with narrow bandwidth carrier tracking filters which might track some other spectral line instead of the carrier.

Other data is also provided. The width of the ellipse along the line $\omega = 0$ is the time resolution capability of the signal while the width along the line $\tau = 0$ is the doppler resolution capability. Furthermore, the three-dimensional representation indicates the signal energy which is shown by the height of the peaks.

Range and velocity accuracy may be predicted from an analysis of the probability of detecting a signal in the presence of noise. Thus in the case of white gaussian noise of power N, the probability of observing y which represents the input signals in the presence of the noise, given s, is given by

$$p(y/s) = k\, e^{-(y-s)^2/2N}. \qquad (3)$$

where k is a normalizing constant. This expression may be expanded and expressed in terms of functions of both time and frequency which lead to an expression involving the ambiguity function in the form of

$$p(\Delta\tau, \Delta f) = k\, e^{2/N_o\ \chi(\Delta\tau, \Delta f)} \tag{4}$$

where N_o is the single-side noise power spectral density. Further manipulations using power series expansions provides the valuable result that the variance of the time measurement is given by

$$\overline{\Delta\tau^2} = \frac{1}{\beta^2\left(\frac{2E}{N_o}\right)} \tag{5}$$

where E is the energy of a signal pulse and β is a mathematical expression analogous to the "moment of inertia" and serves to describe that quality of the signal spectrum. The "rms bandwidth" β is given by

$$\beta^2 = \frac{\int (2\pi f^2) |S(f)|^2\, df}{\int |S(f)|^2\, df} \tag{6}$$

where S(f) is the lowpass equivalent filter function of the signal spectrum. Similarly the variance in the doppler measurement is given by

$$\overline{\Delta f^2} = \frac{1}{t_o^2\left(\frac{2E}{N_o}\right)} \tag{7}$$

where t_o, the "rms time duration" of the signal, is given by

$$t_o^2 = \frac{\int (2\pi t)^2 |\mu(t)|^2\, dt}{\int |\mu(t)|^2\, dt} \tag{8}$$

and $\mu(t)$ is defined above.

In the case of the rectangular pulse a somewhat different analysis is required which gives the results

$$\Delta\tau(\text{rms}) = \frac{1.414\,\tau_p}{\left(\frac{2E}{N_o}\right)} \tag{9}$$

and

$$\Delta f(\text{rms}) = \frac{1}{1.8\,\tau_p\sqrt{\frac{2E}{N_o}}} \tag{10}$$

It will be seen that these theoretical predictions closely approximate the results obtained with practical systems.

Performance of Practical Systems

This section presents mathematical models of the four basic systems and shows briefly how these models are analyzed to obtain predictions of their performance.

As a first step a brief description of each system is given. Then a linear model applicable to all the systems is presented. The noise response of the gating units is then described for the cases of the split gate tracker and the leading edge tracker. Finally the effect of the loop filtering is given for both the noise and dynamic tracking errors.

It should be noted that a complete tracking system contains a signal generator, transmitter, timing reference or oscillator, as well as the receiver, tracking filter, phasemeters, counters, etc. The discussion presented here is limited to the performance of the tracking filter and the effect of the IF filtering on this performance.

Models of the four systems. --Phase-locked loops: In practice the phase-locked loop may be constructed in the simple form of Figure 1 or it may be more complex, having IF amplifiers and mixing stages. And, in certain high dynamic situations two or more loops may be used in combination with one loop providing a rate aiding signal to the second loop. For the purposes of this description it suffices to consider the simple or standard form of the loop.

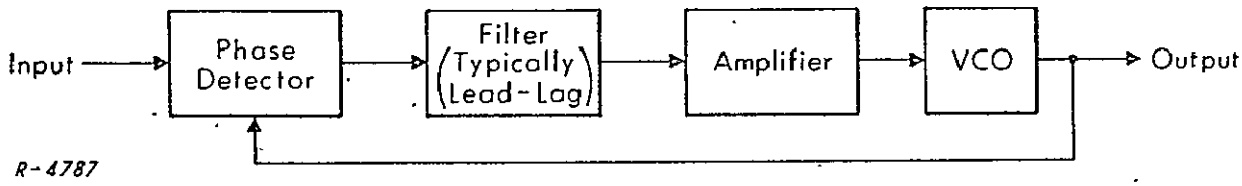

Figure 1 Phase-Locked Loop

The simple loop contains a phase detector, voltage controlled oscillator (VCO) and some form of amplification and filtering to develop a suitable VCO control signal from the phase detector output. The filter and amplifier are usually designed as a single unit, an operational amplifier with an RC feedback network. The filter is designed to optimize some characteristic of the loop performance for the situation in which the loop is to be used. For example, the filtering is frequently designed to minimize the sum of the dynamic and noise induced errors.

Split gate range tracker: This unit has the same general configuration of the phase-locked loop, but some components have been replaced with the corresponding ones for pulse operation. Thus the VCO is replaced with a variable speed clock and gate generator and the phase detector is replaced by a gating unit.

A simple split-gate tracking loop is shown in Figure 2.

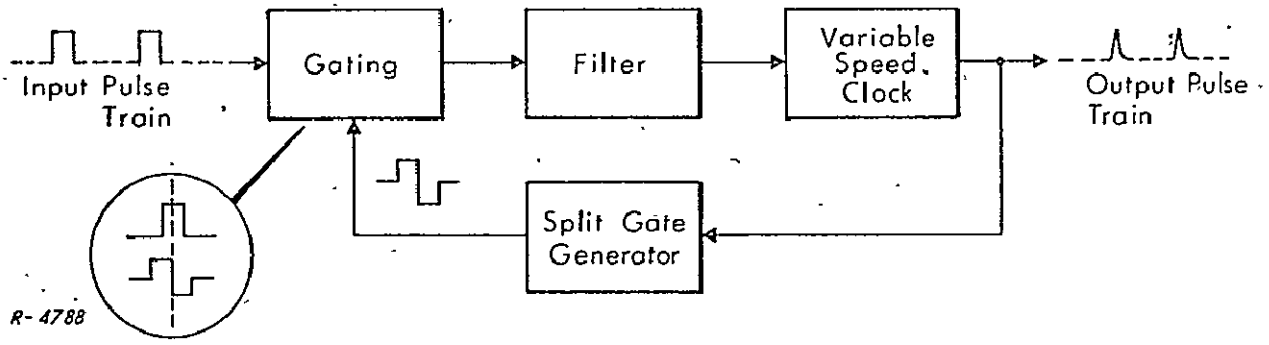

Figure 2 Simple Split-Gate Tracking Loop

The loop accepts the input pulse train and produces an output pulse train which is locked to the input. The loop acts as a smoothing filter which substantially reduces the noise content of the pulse train by reducing the noise bandwidth of the system.

Leading edge range tracker: A simple leading edge tracker is shown in Figure 3. It has the same form as the preceding figure but the gating unit functions differently. This loop responds in the same fashion as that of the split-gate tracker.

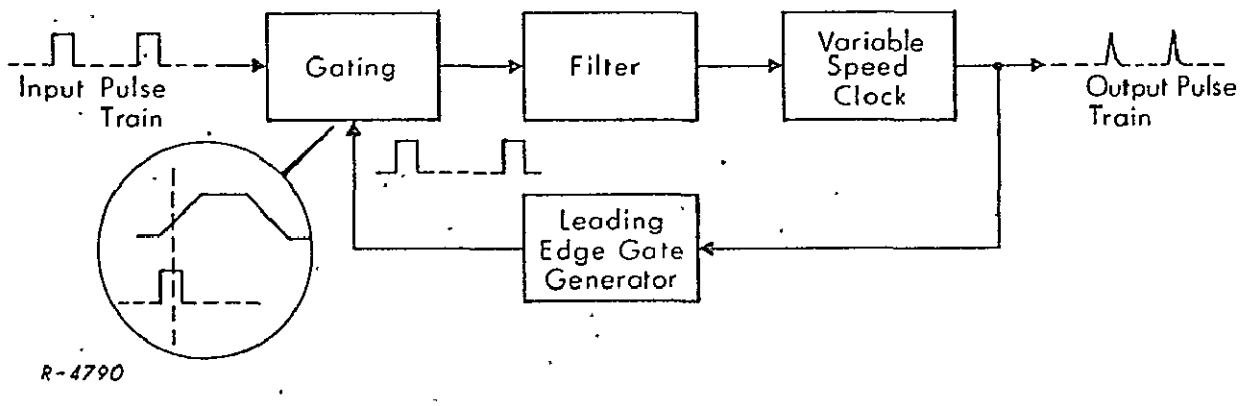

Figure 3 Leading Edge Range Tracker

Harmonic tone ranging system: This system differs from the preceding three systems in that typically a few signals are tracked simultaneously. Thus a system utilizing four ranging tones modulated on to a carrier requires four tracking filters in the receiver. Since each ranging tone is a sinusoid, the phase-locked loop is employed as the tracking filter. A simple system is shown in Figure 4.

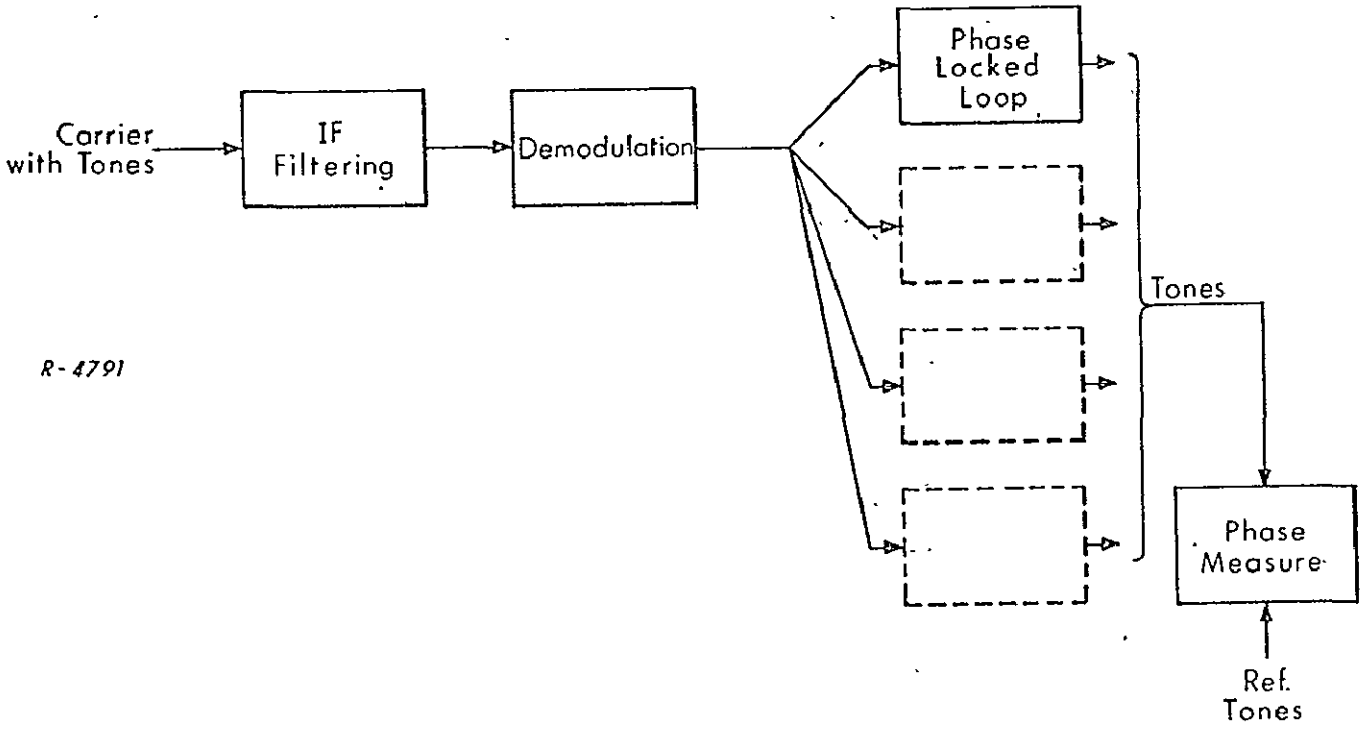

Figure 4 Harmonic Tone Ranging System

In a more complex system, the carrier is also tracked in order to provide highly precise rate aiding signals to each of the phase-locked loops. In such a system the dynamic and noise induced errors are substantially reduced.

Generalized models: The operation of the phase-locked loop, split-gate tracker, and leading edge tracker are very much alike. Thus the function of the phase detector is to provide an error signal which represents the difference in phase between the input and output signals. And similarly the gating unit provides an error signal representing the timing difference between the input and output. Both units function as multipliers and may be represented in linearized models as summing points.

The operation of the VCO or variable speed clock is characterized as an integrator. Its frequency is set at some nominal value for the case of zero error signal. A change in frequency in response to a nonzero error signal is proportional to the error signal. The output phase or time period is related to the integral of the frequency, or equivalently, the integral of the filtered error signal. The effect of the error signal is to drive the loop to null out the input-output error.

The filter is usually a lead lag filter though it is possible to improve the loop performance by including an additional ideal integrator such as may be synthsized digitally. The filter also serves as the connecting link between the split-gate tracker and the phase-locked loop. It provides for the same type operation in both loops even though one loop accepts a pulse input signal while the other accepts a continuous wave. The filter can effect the similarity in operation when its bandwidth is very much smaller than the pulse repetition frequency (PRF). Under this condition the contributions of the pulses in the input pulse train are effectively summed together to form a continuous output from the filter. The continuous output

of the filter in the case of the split-gate tracker is virtually indistinguishable from that of the phase-locked loop. Note further that poisson noise spikes at the input to the filter will result in approximately gaussian noise at the output of the filter.

A single linearized model is applicable to the phase-locked loop, and the split-gate and leading edge trackers. Their configurations may now be recast to show the Laplace transform representation shown in Figure 5 where $T_i(s)$ and $T_o(s)$ refer to the time signals of the split-gate and leading edge signals while $\psi_i(s)$ and $\psi_o(s)$ refer to the phase signals of the phase-locked loop. Thus the loops perform in a similar manner within their linear regions. However, it should be noted that they differ in their acquisition performance since the split-gate and leading edge tracker require a strobing action to locate the input pulse.

In Figure 5, the VCO is shown by the usual representation as an integrator. The constant k includes all gains that may be present such as those of the operational amplifier (not shown) used to drive the VCO, the VCO gain itself, and the gain of the split-gate detector or the phase detector.

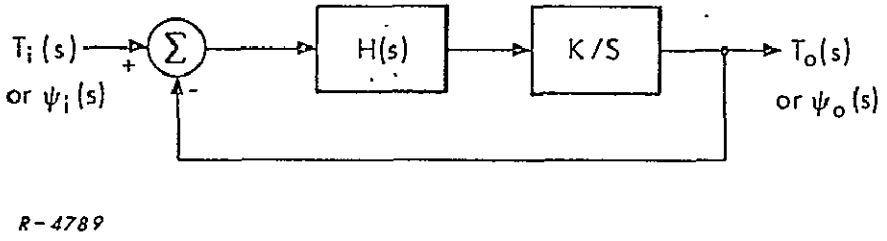

Figure 5 Transform Representation of Tracking Loop

The open loop transfer function for the case where a lead lag filter is employed is given by $(k/s)(\tau_1 s + 1)(\tau_2 s + 1)^{-1}$. Increased performance can be obtained by using a lead filter followed by an additional integrator. Such an integrator can be built by digital techniques. The resulting open loop transfer function is then given by $(k/s^2)(\tau_1 s + 1)$.

For purposes of analysis the tracking loop is generally treated as a filter with input $T_i(s)$ or $\psi_i(s)$ and output $T_o(s)$ or $\psi_o(s)$. The transfer function of this filter is simply the closed loop transfer function of the loop. In the case of the lead lag filter and single integration, it is given by

$$H_L(s) = \omega_n^2 \frac{\tau_1 s + 1}{s^2 + 2\zeta\omega_n s + \omega_n^2} \qquad (11)$$

where $\omega_n^2 = k/\tau_2$ and $2\zeta = \omega_n(\tau_1 + k^{-1})$. In the case of the lead filter and double integration, it is given by Eq. (11) with $\omega_n^2 = k$ and $2\zeta = \omega_n \tau_1$. The exact form of the closed loop response of the tracker determines its dynamic performance and is an important factor in determining its noise performance. These details are discussed in Appendix B for the case of a phase-locked loop and in Appendix C for the split-gate, leading edge and harmonic range tone trackers.

Method for deriving noise and dynamic performance. --The noise and dynamic performance of the phase-locked loop is calculated from Eq. (11) by treating $\psi_i(s)$ as the noise or as a power series representation of the input phase (or range) perturbation. The dynamic response of the split-gate and leading edge trackers is found in a similar way. However, the noise response of the split-gate and leading edge trackers requires calculations of the effect of the gate on the noise. This, in turn, depends on the IF filtering. Thus the response of the split-gate and leading edge trackers to noise is dependent on the gate, the IF filtering, and the loop filtering.

As a first step the effect of the gate on the noise induced error is investigated. Then the effect of the loop filtering on the noise induced error may be found for all the systems. And finally the dynamic performance of the systems is found as a function of the loop filtering.

The error resulting from the noise is a function of both the average noise power and average signal power or simply the signal-to-noise ratio (SNR). Both the gate tracking error signal and the noise disturbance on this signal are functions of the gate width. It is therefore necessary to determine the gate width which minimizes the noise induced error.

The IF filtering similarly plays a role in the gate tracking error and the noise disturbance. The bandpass characteristic of the filter affects the pulse shape and thus the required gate width, as well as the spectral distribution of the noise power. It is therefore convenient to adopt a simple representation for the filtering so that the noise error at the gate may be expressed in terms of a filter parameter.

The instantaneous values of the voltage appearing in the gate are summed together or integrated by the loop filter following the gate so that the only meaningful expression of the gate signal is in the form of an integral. Thus the expression for the noise signal e_n is given by

$$e_n = \int_{-\infty}^{\infty} m(t)\, g(t)\, dt \qquad (12)$$

where $m(t)$ is the instantaneous value of the noise and $g(t)$ the gate function for the split gate and leading edge gate, respectively, is shown in Figures 6 and 8. This expression may be expanded in terms of the autocorrelation function of the noise $R_m(\tau)$ and the gate $R_g(\tau)$ to give

$$\overline{e_n^2} = \int_{-\infty}^{\infty} R_m(\tau)\, R_g(\tau)\, dt \qquad (13)$$

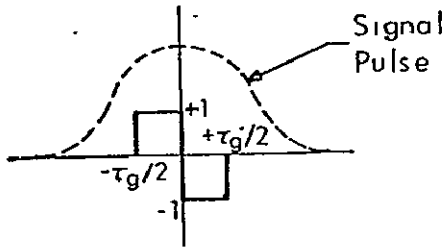

Figure 6 Split Gate

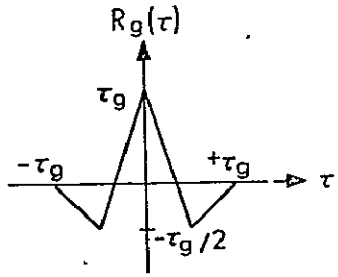

Figure 7 $R_g(\tau)$ Split Gate Correlation Function

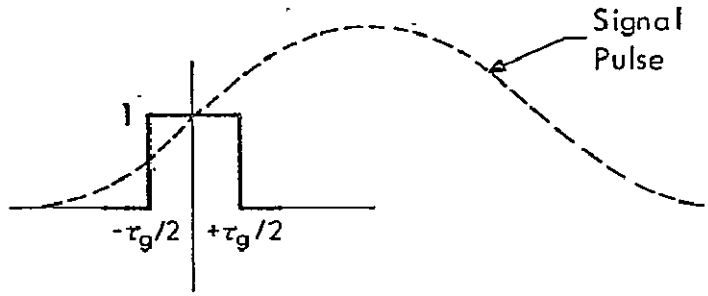

Figure 8 Leading Edge Gate

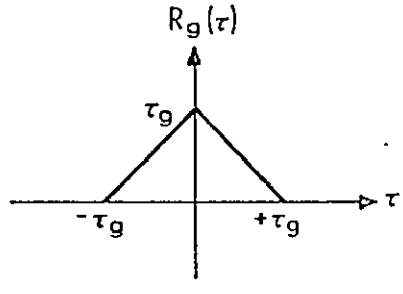

R-4792

Figure 9 $R_g(\tau)$ Leading Edge Correlation Function

which is a convenient expression since $R_m(\tau)$ is readily expressed in terms of the IF bandpass characteristic and $R_g(\tau)$ is given by Figures 7 and 9. For these purposes the IF bandpass characteristic may be expressed in terms of the equivalent single-sided baseband representation which, for demonstration purposes, may be presumed to have a double RC rolloff, $a^2/(s+a)^2$, where $a = 1/RC$. The single-sided bandwidth is equal to 0.65a. Then $R_m(\tau)$ is found by the usual procedure of evaluating the inverse transform of the noise power spectral density function (the squared magnitude of the filter function) for positive values of $s = j\omega$. The result is that e_n can be expressed in terms of the parameters $\underline{a}$ which is the filter corner frequency, τ_g which is the gate width and N_o, the noise power spectral density. Thus,

$$e_n = e_n(a, \tau_g, N_o) \tag{14}$$

The next step in the analysis to to calculate the response of the filter $a^2/(a+s)^2$ to a pulse. For convenience, let the pulse amplitude be given by V_o and the width by τ_p. The signal pulse, P(t), may be expressed as a positive going step plus a negative going step which has been delayed by τ_p seconds. Thus,

$$P(t) = V_o \left[u_{-1}(t) - u_{-1}(t - \tau_p)\right] \tag{15}$$

The response of the filter to the pulse is given by

$$f_{p1}(t) = V_o \Big[\left(1 - e^{-at} - at\, e^{-at}\right) u_{-1}(t) - \left(1 - e^{-a(t-\tau_p)} - a(t-\tau_p)\, e^{-a(t-\tau_p)}\right) u_{-1}(t-\tau_p)\Big] \tag{16}$$

To facilitate the calculations, the waveform of Eq. (16) is approximated by

$$f_p(t) = 0.4\, V_o \left(1 + \cos \frac{\pi a}{3.5}\, t\right) \tag{17}$$

for the case of the split-gate tracker with $\tau_p = 3/a$, and by

$$f_p(t) = \sin^2(\pi a t/8) \tag{18}$$

which approximates the leading edge of the pulse for $\tau_p \geq 6/a$ in the case of the leading edge tracker. The value $\tau_p = 3/a$ is chosen to provide a fairly symmetrical pulse to the split-gate. The symmetry is desirable from the point of view that the ideal filter (the matched filter) produces a symmetrical triangular pulse. The value $\tau_p = 6/a$ is chosen since the rise time and the form of the leading edge is essentially unchanged for longer pulse widths or wider filter bandwidths.

The gate error signal, in the absence of noise, is zero when the gate is correctly positioned in time with respect to the signal pulse. When the gate is displaced relative to the pulse by a displacement Δt, a nonzero error signal is developed. By analogy with Eq. (12) the error signal e_e is also expressed by an integral expression involving the gate minus the integral of a reference signal. In the case of the split-gate, the reference is taken as zero. In the case of the leading edge gate, the reference is taken as equal to the gate voltage for $\Delta t = 0$. Thus the gate error signal is given by

$$\begin{aligned} e_e &= \int_{-t_g/2+\Delta t}^{\Delta t} f_p(t)\, dt - \int_{\Delta t}^{\Delta t+\tau_g/2} f_p(t)\, dt \\ &= e_{es}(V_o, a, \tau_g, \Delta t) \end{aligned} \tag{19}$$

for the split gate with $f_p(t)$ given by Eq. (17) and by

$$e_e = \int_{T_o-\tau_g/2+\Delta t}^{T_o+\tau_g/2+\Delta t} f_p(t)\,dt - \int_{T_o-\tau_g/2}^{T_o+\tau_g/2} f_p(t)\,dt$$

$$= e_{e\ell}(V_o, a, \tau_g, \Delta t) \tag{20}$$

for the leading edge gate with $f_p(t)$ given by Eq. (18) and where T_o represents the time of occurrence of the center of the gate when the gate is correctly positioned relative to the signal pulse.

The final step in evaluating the effect of the gate on the noise induced error is to determine how much error signal e_e is required to balance out e_n. Therefore set

$$\left.\begin{aligned} e_{es}(V_o, a, \tau_g, \Delta t) &= e_{ns}(a, \tau_g, N_o) \\ e_{e\ell}(V_o, a, \tau_g, \Delta t) &= e_{n\ell}(a, \tau_g, N_o) \end{aligned}\right\} \tag{21}$$

where the subscripts s and ℓ stand for split-gate and leading edge gate. The term Δt may be factored out. Then replacing Δt with the rms timing error σ_t and solving for σ_t gives

$$\sigma_{t_{min}} = \frac{1.56}{a\sqrt{E/N_o}} \tag{22}$$

for the split-gate and

$$\sigma_{t_{min}} = \frac{3.1}{a\sqrt{E/N_o}} \tag{23}$$

for the leading edge gate. The subscript min indicates that the expressions of Eq. (21) have been evaluated for the value of $a\tau_g$ which minimizes the expression for σ_t. The minimum value of σ_t is obtained for $a\tau_g \approx 4.5$ for the split-gate, and $a\tau_g \approx 1$ for the leading edge gate. The symbol E represents the energy in the signal pulse before the IF filter. In the case of the leading edge gate, E represents the energy in a pulse of duration $\tau_p = 6/a$.

So far, the effect of the gate in the split-gate tracker and the leading edge tracker has been considered. Now the effect of the loop filtering can be considered for the cases of all four systems.

The noise response of the phase-locked loop may be evaluated directly by treating it as a filter whose transfer function is given by Eq. (11). Thus the noise voltage at the filter output is given in transform notation by

$$\psi_{en}(s) = H(s)\, \psi_n(s) \tag{24}$$

where $\psi_n(s)$ represents the phase noise input. The input phase noise, Ψ, may be related to the additive white noise density, $\Phi = N_o$, through an analysis of the operation of the input mixer. This analysis is performed in Appendix B where it is shown that

$$\Psi = \frac{N_o}{2S} \tag{25}$$

where S is the average power of the input sinusoid. In terms of the loop noise bandwidth B_n the error may be expressed as

$$\phi_n(\text{rms}) = (\Psi B_n)^{1/2} = \left(\frac{2S}{N}\right)^{-1/2}_{B_n} \tag{26}$$

where the SNR is measured in the loop bandwidth.

A similar result is obtained for each tone of a harmonic tone ranger. However, the precision of the measurement based on all the tones is increased when the signal spectrum has been designed so that the spectral lines fall near the outer edge of the spectrum. For such a system the error is decreased by a factor of $\sqrt{n}$ where n is the number of tones.

Expression for the noise and dynamic errors. --For a phase-locked loop the noise error in the range measurement is given by

$$\sigma_R = \frac{c}{4\pi f} \left(\frac{2S}{N}\right)_{B_n}^{-1/2} \tag{27}$$

where c is the speed of light and f is the frequency of the tone or of the carrier, whichever is the input sinusoid. The factor of 4 is present with a two-way range measurement. A factor of 2 is present with a one-way range measurement.

For an n-tone harmonic ranging system (the simple form without rate aiding signals from the carrier) the range error is given by

$$\sigma_R = \frac{c}{4\pi f} \left(\frac{2nS}{N}\right)_{B_n}^{-1/2} \tag{28}$$

In the case of sample data systems, such as the split-gate range tracker and the leading edge range tracker, the loop filtering provides an improvement in the precision of the measurement by a factor equal to the square root of the number of input data pulses for each sample of the output. The output data sample rate is limited by the loop bandwidth in accordance with the sampling theory. The optimized range

error is given by

$$\sigma_R = \frac{1.56\ c}{a\sqrt{E/N_o}\ \sqrt{f_r/2B_n}}$$

$$= \frac{1.56\ c}{a}\left(\frac{S}{N}\right)_{B_n}^{-1/2} \tag{29}$$

for the split gate range tracker where the term f_r is the pulse repetition frequency and B_n is the single-sided noise bandwidth. Similarly,

$$\sigma_R = \frac{3.1\ c}{a}\left(\frac{S}{N}\right)_{B_n}^{-1/2} \tag{30}$$

for the leading edge range tracker.

The dynamic tracking errors are determined by the loop bandpass characteristic since the IF filtering is sufficiently wideband to have no more than a negligible effect. Thus the expressions for the dynamic tracking errors are the same for each system. In accordance with the representation of Figure 5, the dynamic tracking error $T_e(t)$ is given by

$$T_e(t) = T_i(t) - T_o(t) = \mathcal{L}^{-1}\left\{T_i(s)[1 - H_L]\right\} \tag{31}$$

where $H_L(s)$ is given by Eq. (11). Let the input be represented by a power series

$$T_i(t) = T_i(o) + \alpha t + \beta\left(\frac{t^2}{2}\right) + \gamma\left(\frac{t^3}{6}\right) \tag{32}$$

For a loop containing a lead lag filter and a single integration, the tracking error in response to the input power series is given by

$$T_e(t) = \left[\frac{\alpha}{k} + \frac{\beta}{\omega_n^2} - \frac{\gamma(k\tau_1+2)}{k\omega_n^2}\right] + \left[\frac{\beta}{k} + \frac{\gamma}{\omega_n^2}\right] t + \left(\frac{\gamma}{k}\right)\left(\frac{t^2}{2}\right) + \text{transients} \tag{33}$$

in which a small approximation has been made on the assumption that $\tau_2 >> \tau_1$, and $k >> 1$. The transients die out within a short time inverval on the order of the reciprocal of the loop bandwidth. In most applications, they can usually be neglected.

For a tracking loop containing a lead filter and a double integration, the steady state tracking error in response to the input power series is given by

$$T_e(t) = \left[\frac{\beta}{k} - \frac{\gamma\tau_1}{k}\right] + \frac{\gamma}{k}\, t \tag{34}$$

which shows that a double integration reduces the powers of t in the expression for the dynamic error.

These dynamic tracking expressions have been written in terms of the parameter $T_i(t)$ the input time modulation. They may be converted to range by multiplication by the factor, c, the speed of light.

Appendix A

FUNDAMENTAL THEORY

This section presents the theoretical aspects of range measurement. The theory is basic to radar ranging techniques in which the time of signal propagation over the unknown distance is measured. The results of the theory are equally applicable to signals transmitted at the low and high frequency portions of the electromagnetic spectrum because the derivations are, for the most part, only concerned with baseband signal representations. The results are directly applicable to laser ranging devices except in some cases where the character of the noise of the optical detection process must be considered.

The discussion below treats the classical radar problem of obtaining the best ranging accuracy for a given signal waveform in the presence of Gaussian noise. The relationship between the signal spectrum, the receiver filtering and the ranging accuracy is developed so that both the signal waveform and the receiver can be designed for best accuracy. The results of the theoretical analysis are compared in Appendix C, with the performance obtained from practical range tracking systems where it is shown that near optimum performance is obtained with these systems.

The discussion begins with signal reception and detection by matched filters. This is followed by a discussion of ambiguity functions, and the attainable accuracy of range and velocity measurements. Particular reference is given to the special case of rectangular pulse signal.

Matched Filters

A generalized receiver is shown in Figure A-1.

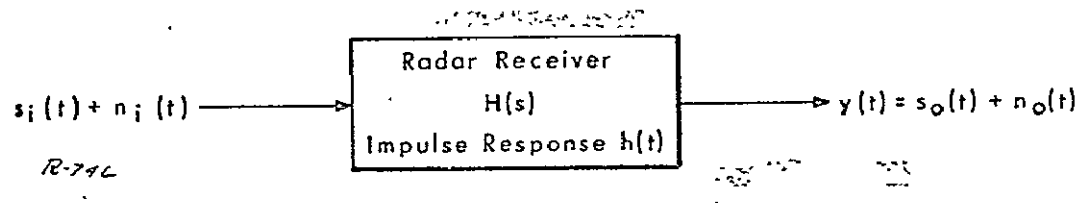

Figure A-1 A Model of a Radar Receiver

For simplicity the mixing operations, input filtering, etc., are not shown. In this simplified representation it is assumed that the receiver subjects the incoming signal $s_i(t)$ plus noise $n_i(t)$ to a linear filtering process represented by H(s) or h(t). The problem is to determine the specific form of h(t) which maximizes the SNR at the output of the filter at a given sampling time $t = \tau$.

The solution to this optimization problem for the case when $n_i(t)$ is additive white gaussian noise is well known. The optimum linear system, H(s), is a matched filter, sometimes called a correlation detector. Note that this solution has wide application since, in most cases, receiver input noise can be reasonably described as additive white gaussian noise.* The derivation of the optimum filter for this case is included here because of its almost universal applicability.

With reference to Figure A-1, it is desired to maximize the ratio of the square of the value of the signal component at $t = \tau$,

$$s_o^2(\tau) = \left[\int_0^\tau s_i(t)\, h(\tau - t)\, dt\right]^2,$$

to the expected value of the noise power, $E[n_o^2(t)]$.** Let this ratio be denoted by R; then

$$R = \frac{\left[\int_0^\tau s_i(t)\ h(\tau - t)\ dt\right]^2}{E\left[\int_0^\tau n(t)\, h(\tau - t)\ dt\right]^2} \qquad \text{(A-1)}$$

It is assumed in Eq. (A-1) that the noise is wide-sense stationary with zero mean. Since the noise is white, its autocorrelation is an impulse

---

*Note that given enough smoothing Poisson noise takes on gaussian characteristics.

**$E[f(t)]$ is read as "the expected value of f(t)."

function so that

$$E[n_o^2(\tau)] = \int_0^\tau \int_0^\tau n_i(t_1)\, n_i(t_2)\, h(\tau - t_1)\, h(\tau - t_2)\, dt_1\, dt_2$$

$$= \int_0^\tau \int_0^\tau \frac{1}{2} N_o\, \delta(t_1 - t_2)\, h(\tau - t_1)\, h(\tau - t_2)\, dt_1\, dt_2$$

$$= \frac{N_o}{2} \int_0^\tau h^2(\tau - t)\, dt \qquad (A\text{-}2)$$

N_o is the power spectral density of the input noise.* Substituting Eq. (A-2) in Eq. (A-1) and dividing both sides by the input signal energy, $E_o = \int_0^\tau s_i^2(t)\, dt$, Eq. (A-1) becomes,

$$\frac{N_o R}{2E_o} = \frac{\left[\int_0^\tau s_i(t)\, h(\tau - t)\, dt\right]^2}{\int_0^\tau s_i^2(t)\, dt \int_0^\tau h^2(\tau - t)\, dt} \qquad (A\text{-}3)$$

At this point the Schwartz Inequality is invoked which says that for any two functions a(t), b(t),

$$\left(\int a(t)\, b(t)\, dt\right)^2 \le \int a^2(t)\, dt \int b^2(t)\, dt \qquad (A\text{-}4)$$

The equality holds when $a(t) = kb(t)$, where k is a constant. With reference to Eq. (A-3), this means that the maximum signal-to-noise at the output of the receiver is obtained (at time $t = \tau$) when $h(\tau - t) = s_i(t)$ to within an unimportant nonzero scale factor, k. Simply stated, the impulse response of the optimum linear system is the mirror image of the input waveform, shifted to the right by the time duration, τ, of the signal.

*Single-side spectra are assumed throughout this report.

The filter frequency function is, then, the complex conjugate of the signal spectrum, with an additional linear phase shift $\omega\tau$. The receiver output at $t = \tau$ is expressed as

$$s_o(\tau) = \int_0^{\tau} s_i(t)\, s_i(t)\, dt \qquad \text{(A-5)}$$

and the output of the detector at some intermediate time, t, $0 \le t \le \tau$, is

$$s_o(\tau) = \int s_i(\sigma)\, s_i(t + \sigma)\, d\sigma \qquad \text{(A-6)}$$

hence the name correlation detection.

The presence or absence of a target-returned signal is determined by subsequent operations on $y(t) = s_o(t) + n_o(t)$. If y(t) is above a threshold y_o it is decided that a target is present, below y_o it is decided that there is no target. The exact level of the threshold is fixed by trading off the probability of detection of a target in a noisy environment against the probability of false alarm. As the threshold is raised it becomes less likely that the noise alone will exceed the threshold and cause a false alarm. At the same time, it becomes less likely that the signal and noise will exceed the threshold when a target is present. Curves of probability of detection versus probability of false alarm with signal-to-noise ratio as a parameter are available in the literature (Ref. 1, 2). One such set of curves is reproduced in Figure A-2. These curves represent an upper bound. Results obtained with a less than optimum receiver lie below and to the right of these curves. The parameter R in this set of curves is equal to the ratio of the target echo signal energy to the effective input noise power/Hz. The solid lines represent the results obtained with a target echo of constant amplitude. The dotted lines represent the results obtained with a fluctuating target amplitude which varies in accordance with a Rayleigh distribution. In this case the parameter R is given by A_o^2/N_o where A_o is the most probable amplitude.

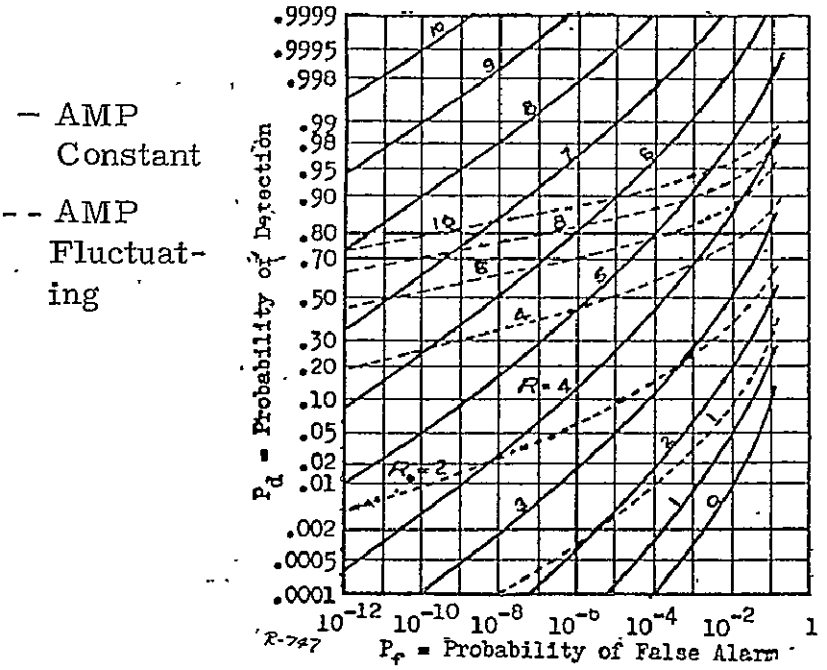

Figure A-2 Receiver Detection Characteristics

Ambiguity Diagrams

So far, it has been shown that a receiver that is matched to the transmitted signal waveform is optimum because it maximizes the signal-to-noise ratio of its output at $t = T$. However, no restrictions were placed on waveform design. This points up a very important generalization. When the receiver is matched to the signal input, the detectability of that signal is a function only of the signal energy received, E_o, and the noise figure of the receiver as expressed by, N_o, the noise power spectral density. Signal design is important to the trajectory parameter measurement process, namely the measurement of the range and velocity of the target. One indicator of the utility of a particular signal design is its ambiguity diagram. (Ref. 3) An ambiguity function represents the envelope of the response of a correlation receiver to inputs that are mismatched due to doppler shifts. The ambiguity function is just the magnitude of correlation of the complex envelope (Ref. 4) $\mu(t)$ of the input signal, s(t), with the doppler shifted complex envelope. That is,

$$\chi(\tau,\omega) = \left| \int_{-\infty}^{\infty} \mu(t)\, \mu^*(t+\tau)\, e^{j\omega t} dt \right| \qquad (A-7)$$

An ambiguity diagram is the 3 dB contour of the ambiguity function. The width of the diagram along the line $\omega = 0$ is the time resolution capability of the signal. Similarly, the width along the $\tau = 0$ line is the doppler resolvability of the signal. Examples of ambiguity functions and diagrams are numerous in the literature (Refs. 1, 3). The ambiguity diagrams for a signal consisting of one pulse of RF and a signal consisting of several pulses are shown in Figure A-3.

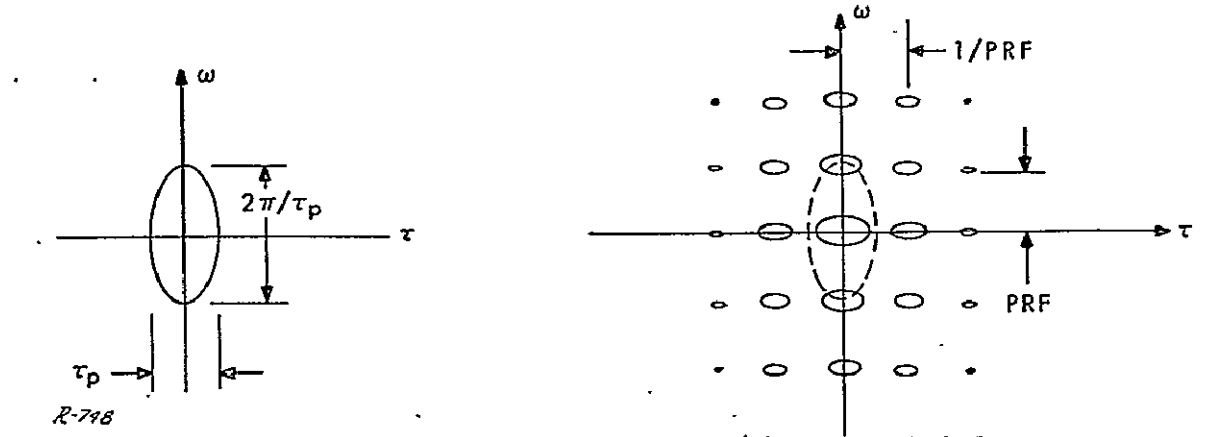

(a) Single Pulse (b) Several Pulses

Figure A-3 Some Ambiguity Diagrams

For one pulse of duration τ_p sec, the width along $\omega=0$ is τ_p and the width along $\tau=0$ is $1/\tau_p \approx$ Bandwidth. Examination of the diagram for several pulses explains the source of the term, ambiguity. In this case, the ambiguity function which contained a single peak breaks up into many peaks. The ambiguity diagram thus displays the "once around again" range ambiguities in the τ direction, and the doppler ambiguities caused by the line spectrum of the signal in the ω direction.

In addition to containing the resolvability and ambiguity properties of a particular signal, the ambiguity diagram also indirectly contains information about the attainable accuracies in range and doppler for a given waveform. This is a result of the fact that the optimum accuracies are a function of the input signal-to-noise ratio and the signal's resolution capabilities which are displayed in the ambiguity diagram.

Range and Velocity Accuracy

The estimation of range and velocity of a radar target involves the evaluation of the probability of receiving a particular radar return in a noise environment. Let p(s) be the probability density of a particular signal and p(y) be the probability of receiving a particular signal, s, in the presence of the noise, n. The joint probability density of signal and

noise plus signal is expressed in terms of conditional probabilities.

$$p(s,y) = p(s)\,p(y/s) = p(y)\,p(s/y) \qquad \text{(A-8)}$$

where $p(y/s)$ is read as "the probability of event y given s". Since y is a given event, i.e., the received data, let $p(y)$ = constant = $1/k$. Equation (A-8) reduces to

$$p(s/y) = kp(s)\,p(y/s) \qquad \text{(A-9)}$$

This equation describes the operation of an ideal observer (Refs. 3, 5) who determines that a particular signal (with particular time delay and doppler shift) was received given the actual signal and noise, y, at the receiver output. When n is gaussian noise, the probability of observing y given s is

$$p(y/s) = k\,e^{-(y-s)^2/2N} \qquad \text{(A-10)}$$

where c is a normalizing constant and N is the noise power output of the receiver. The ideal observer observes y and computes the probabilities

$$p(s_n/y) = k\,p(s_n)\,e^{-(y-s_n)^2/2N} \quad (n = 1, 2, \ldots) \qquad \text{(A-11)}$$

where the s_n represent the various undisturbed signals, one of which is likely to be present in y(t). The ideal observer then simply chooses the most likely "s_i given y" and decides that $y = s_i + n$. When y, n, and s are functions of time, Eq. (A-11) becomes

$$\begin{aligned} p(s/y) &= k\,p(s)\,e^{-\frac{2}{N_o}\int (y-s)^2 dt} \\ &= k\,p(s)\,e^{-\frac{2}{N_o}\left[\int y^2 dt + \int s^2 dt - 2\int y\,s\,dt\right]} \end{aligned} \qquad \text{(A-12)}$$

where N_o is again the single-sided noise power spectral density. When the signal is properly acquired by the receiver, the integrals of y^2 and s^2 over time are independent of particular time delays and doppler shifts, the parameters of interest. It is possible, then, to absorb the contributions of these terms into the normalizing constant, k. It is also reasonable to assume that the probability of receiving a signal with a particular time delay and doppler shift is constant in the range of time delays and doppler shifts under consideration here; i.e., the regions over which all time delays and doppler shifts are considered equally likely is much wider than

the range of time delay and doppler measurement accuracies. Equation (A-12) reduces to

$$p(s/y) = k\, e^{+\frac{4}{N_o} \int s(t)\, y(t)\, dt} \qquad \text{(A-13)}$$

Again, Eq. (A-13) shows that the ideal observer performs a correlation of the received waveform y(t) with the expected waveform s(t). But, this result is stronger. Whereas the previous argument showed that the matched filter was the best linear system for the detection of signal in white gaussian noise, the argument leading to Eq. (A-13) applies to all systems, linear and nonlinear, and shows that the best system is the linear one defined by the matched filter.

Now, s(t) is the expected radar return. Therefore, it is a function of some time delay τ_1 and some doppler shift f_1. To include this information, let $s(t) = s(t, \tau_1, f_1)$. Similarly, y(t) is the actual return with time delay τ_2 and doppler shift f_2, with noise added. Therefore, let $y(t) = s(t, \tau_2, f_2) + n(t)$. At this point, it is assumed that the signal-to-noise ratio is large and consequently n(t) is neglected, $y(t) \approx s(t, \tau_2, f_2)$. This is a rather confusing point. If the noise term is neglected, why is there any error in parameter measurement? What happens here is this: Although the noise term itself is neglected, the presence of noise is still manifested in the form of the operation performed by the ideal observer, i.e., Eq. (A-13). As Woodward (Ref. 3) describes it; "We have placed ourselves in the position of an ideal observer who expects noise, but, without realizing it, fails to get any." Thus, Eq. (A-13) reduces to

$$p(\tau_1, f_1 \mid \tau_2, f_2) = k\, e^{+\frac{4}{N_o} \int s(t, \tau_1, t_1)\, s(t, \tau_2, f_2) dt} = +k e^{+\frac{4}{N_o} \phi(\tau_1, f_1, \tau_2, f_2)} \qquad \text{(A-14)}$$

where $\phi(\tau_1, f_1, \tau_2, f_2) = \int s(t, \tau_1, f_1) s(t, \tau_2, f_2)\, dt$. When s(t) is a narrowband function, Eq. (A-14) can be written in terms of $\Delta t = \tau_1 - \tau_2$ and $\Delta f = f_1 - f_2$.

$$p(\Delta\tau, \Delta f) = k\, e^{+\frac{4}{N_o} \phi(\Delta\tau, \Delta f)} \qquad \text{(A-15)}$$

After some manipulation, and an integration over the "fine structure" of s(t) (Ref. 6) it is found that

$$p(\Delta\tau, \Delta f) = k\, e^{+\frac{2}{N_o} \chi(\Delta\tau, \Delta f)} \qquad \text{(A-16)}$$

where $\chi(\Delta\tau, \Delta f)$ is the ambiguity function of the signal s(t), Eq. (A-7).

Now, $\chi(\Delta\tau, \Delta f) = 2|\phi_c(\Delta\tau, \Delta f)|$ can be expanded using the following formula (Ref. 6)

$$|f(x_i)| = f(0) + \mathrm{Re}\sum_i \frac{\partial f(0)}{\partial x_i}\, dx_i + \frac{1}{2}\,\mathrm{Re}\sum_{i,j}\left(\frac{1}{f(0)}\,\frac{\partial f(0)}{\partial x_i}\cdot\frac{\partial f^*(0)}{\partial x_j} + \frac{\partial^2 f(0)}{\partial x_i \partial x_j}\right) dx_i\, dx_j + \ldots. \qquad \text{(A-17)}$$

After some algebra, it is found that

$$\frac{2}{N_o}\chi(\Delta\tau, \Delta f) \underset{ke}{\qquad} \underset{= ke}{\frac{4}{N_o}}\left[\phi_c(0,0) - \frac{1}{2}A_{11}(\Delta\tau)^2 - \frac{1}{2}A_{22}(\Delta f)^2 - A_{12}\Delta\tau\Delta f + \ldots\right] \qquad \text{(A-18)}$$

where

$$A_{11} = \int (2\pi f)^2 |S(f)|^2\, df = \frac{E\beta^2}{2}, \qquad S(f) = \text{Lowpass equivalent filter function}$$

and

$$\beta^2 = \frac{\int (2\pi f)^2 |S(f)|^2 df}{\int |S(f)|^2 df}, \qquad E = 2\int |S(f)|^2 df \qquad \text{(A-19)}$$

Similarly

$$A_{22} = \int (2\pi t)^2 |\mu(t)|^2\, dt = \frac{Et_o}{2}$$

where $\mu(t)$ is defined above, and

$$t_o^2 = \frac{\int (2\pi t)^2 |\mu(t)|^2 dt}{\int |\mu(t)|^2 dt} \qquad \text{(A-20a)}$$

and

$$A_{12} = \mathrm{Re}\int \dot{\mu}(t)\,\mu^*(t)\,(2\pi j t)\, dt. \qquad \text{(A-20b)}$$

By integrating the expanded form of $p(\Delta\tau, \Delta f)$ over Δf, the variance in time measurement is found to be

$$\overline{\Delta\tau^2} = \frac{N_o}{4A_{11}} = \frac{1}{\beta^2 \left(\frac{2E}{N_o}\right)}, \quad A_{12} = 0 \qquad \text{(A-21a)}$$

Similarly integrating over $\Delta\tau$, the doppler error is found to be

$$\overline{\Delta f^2} = \frac{N_o}{4A_{22}} = \frac{1}{t_o^2 \left(\frac{2E}{N_o}\right)}, \quad A_{12} = 0 \qquad \text{(A-21b)}$$

The A_{12} term contains information about the dependence of time errors on doppler errors. In most cases, the two types of errors are independent, $A_{12} = 0$, and all higher-order terms are negligible. Under these conditions

$$p(\Delta\tau, \Delta f) = k e^{\frac{2}{N_o} \chi(\Delta\tau, \Delta f)} = k_o e^{-\frac{1}{2}A_{11}(\Delta\tau)^2 - \frac{1}{2}A_{22}(\Delta f)^2} = P_1(\Delta\tau)P_2(\Delta f) \qquad \text{(A-22)}$$

In some importnat instances (such as "chirp" type signals or "linear FM" waveforms) A_{12} is large. In such cases, it is true that a time error could be mistaken for a frequency error, and the results expressed in Eq. (A-21) are incomplete.

Accuracy Obtained With Rectangular Pulse

In one important case--that of a rectangular pulse--the results derived above do not work even though the delay and doppler errors are independent and $A_{12} = 0$. If the spectrum of a rectangular pulse is inserted in Eq. (A-19), it is found that β^2 is infinite, which would mean that the variance of range measurement goes to zero in accordance with Eq. (A-21). This fallacy results from the fact that the expansion of $\chi(\Delta\tau, \Delta f)$, Eq. (A-17), actually breaks down for a rectangular pulse. Mannassa (Ref. 6) has resolved this difficulty by using a different expansion of $\chi(\Delta\tau, \Delta f)$ which is valid for a rectangular pulse s(t). The results he obtains are as before for the doppler error, i. e,

$$\Delta f(\text{rms}) = \frac{1}{t_o \sqrt{\frac{2E}{N_o}}} = \frac{1}{1.8\tau_p \sqrt{\frac{2E}{N_o}}} \qquad \text{(A-23)}$$

where τ_p is the pulse duration. However, in place of zero for the error in time measurement, he obtains

$$\Delta\tau(\text{rms}) = \frac{1.414\tau_p}{\left(\frac{2E}{N_o}\right)} \qquad \text{(A-24)}$$

Appendix B

THE PHASED-LOCKED LOOP

Introduction

The phase-lock loop (PLL) is a tracking filter. It produces a constant amplitude output waveform which contains a filtered replica of the phase of the input signal. The phased-locked loop finds important applications in the situations where the input signal is obscured by noise and it is desired to obtain a precise duplicate of the phase information carried by the signal Typically, the input noise spectrum is very much wider than the loop noise bandwidth so that the loop is able to filter out a major portion of the noise. This filtering action provides for a precise retrieval of the phase information in the presence of noise. On the other hand, too much filtering will cause a loss of precision because the loop will smooth out fast fluctuations in the input phase information. Thus, the loop bandwidth is usually selected on the basis of a trade off of noise and dynamic error requirements. The relationship between noise and dynamic errors and acquisition performance are derived and discussed below.

In practice the phase-locked loop may be constructed in the simple form of Figure B-1, or it may be more complex having IF amplifiers and mixing stages. And in certain high dynamic situations two or more loops may be used in combination with one loop providing a rate aiding signal to the second loop. For the purpose of this description it suffices to consider the simple or standard form of the loop.

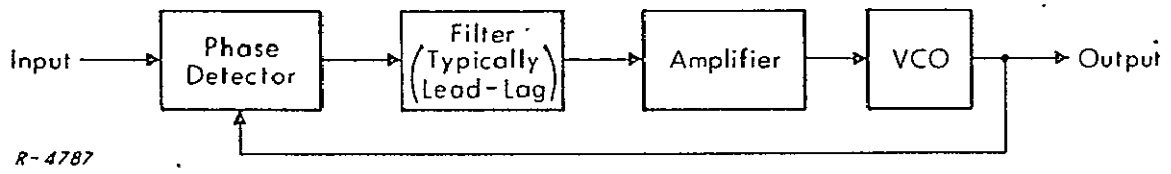

Figure B-1 Phase-Locked Loop

The simple loop contains a phase detector, voltage controlled oscillator (VCO) and some form of amplification and filtering to develop a suitable VCO control signal from the phase detector output. The filter and amplifier are usually designed as a single unit, e. g., an operational amplifier with an RC feedback network. The filter is designed to optimize some characteristic of the loop performance for the situation in which the loop is to be used. For example, the filtering is frequently designed to minimize the sum of the dynamic and noise induced errors, as noted above.

The function of the phase detector is to provide an error signal which represents the difference in phase between the input and output signals. For purposes of analysis it may be regarded as a multiplier, which in a linearized model is represented as a phase summing point. This representation is derived below.

The VCO functions as a phase integrator. Its frequency is set at some nominal value for the case of zero error signal. A change in its frequency in response to a non-zero error signal is proportional to the error signal. The output phase is related to the integral of the frequency or equivalently the integral of the filtered error signal.

Development of a Phase Transfer Model

Consider a CW signal and noise as additive, uncorrelated, inputs to a phase-locked loop. The noise is assumed to be a sample function of a narrow-band zero-mean, Gaussian random process. For convenience, the noise is decomposed into cophasal and quadrature components with the signal phase as reference. Thus, the composite input to the loop is given by

$$e_{in}(t) = E_s \sin[\omega_s t + \phi_s(t)] + x_c(t) \sin[\omega_s t + \phi_s(t)] + x_q(t) \cos[\omega_s t + \phi_s(t)] \tag{B-1}$$

where $x_c(t)$ and $x_q(t)$ are low-pass narrow-band Gaussian processes while the VCO output signal is represented by

$$e_{osc}(t) = \cos[\omega_s t + \phi_o(t)] \tag{B-2}$$

The operation of the phase detector in the loop can be represented as multiplying the input and VCO signals. High frequency components will not be considered since they are filtered within the loop. The phase

detector output is then

$$e_d(t) = E_s\left\{\left[1+\frac{x_c(t)}{E_s}\right]\sin\left[\phi_s(t)-\phi_o(t)\right]+\frac{x_q(t)}{E_s}\cos\left[\phi_s(t)-\phi_o(t)\right]\right\} \tag{B-3}$$

and under small locking error conditions this equation may be linearized to

$$e_d(t) \approx E_s\left\{\left[1+\frac{x_c(t)}{E_s}\right]\left[\phi_s(t)-\phi_o(t)\right]+\frac{x_q(t)}{E_s}\right\} \tag{B-4}$$

so that the phase transfer behavior for the phase detector may be characterized by Figure B-2, provided that $[\phi_s(t) - \phi_o(t)]$ is sufficiently small. Furthermore, if the S/N ratio is assumed large enough then the cophasal component of the noise $x_c(t)$ will have a secondary effect and may be neglected. Thus, under high S/N and small phase-error conditions the phase detector output may be written as

$$e_d(t) \approx E_s\left\{\phi_s(t) - \phi_o(t) + \frac{x_q(t)}{E_s}\right\} \tag{B-5}$$

and the incremental phase-transfer behavior of the loop can be characterized by the linear model of Figure B-3. Note that the incremental output phase of the VCO is obtained by integrating (and scaling) its input excitation. The following notation is used in Figure B-3, referring to the frequency domain:

$\Psi_{in}(s) \equiv \Psi_s(s) + \Psi_n(s)$ represents the composite phase input to the loop, where $\Psi_s(s)$ corresponds to the signal term $\phi_s(t)$ and $\Psi_n(s)$ to the noise term $\frac{x_q(t)}{E_s}$,

$\Psi_o(s)$ represents the VCO phase output,

$\Psi_e(s) \equiv \Psi_s(s) - \Psi_o(s)$ represents the signal locking error in the loop, which must be kept small for the model to be valid,

F(s) represents the low-pass loop filter, and

K represents the open-loop gain in the model, and is proportional to the signal level E_s, and the gains of the phase detector, loop operational amplifier and VCO.

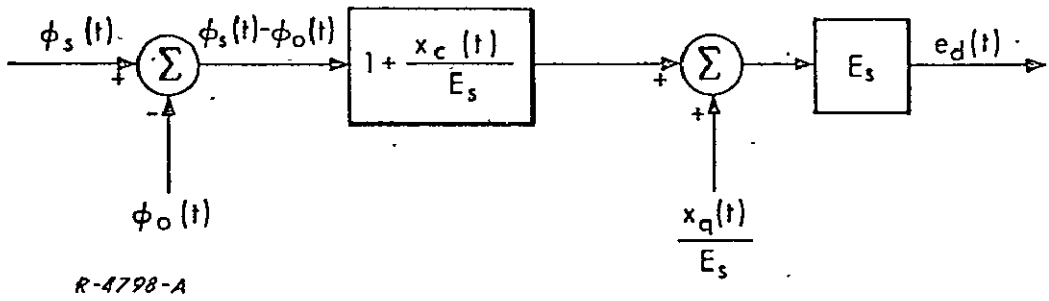

Figure B-2 Phase-Detector Characterization (Small Error Conditions)

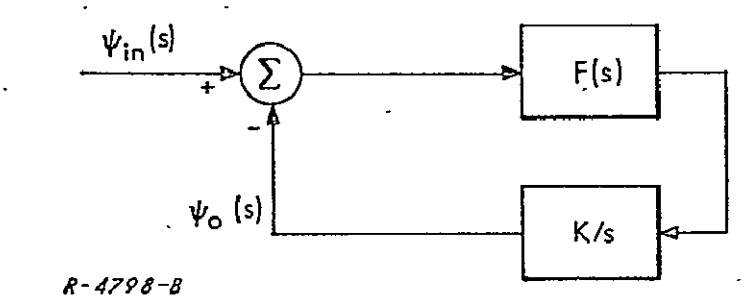

Figure B-3 Linear Phase Transfer Model of a PLL (Small Error, High SNR Conditions)

Phase-Error Analysis

The derivation of the linear model of Figure B–3 required a small signal locking error. If H(s) represents the closed-loop transfer function in the model; i. e.,

$$H(s) = \frac{\psi_o(s)}{\psi_{in}(s)} \tag{B-6}$$

then the expression for this error is given by

$$\psi_e(s) = [1 - H(s)]\ \psi_s(s) - H(s)\ \psi_n(s) \tag{B-7}$$

The first term represent the loop locking error in attempting to reproduce the signal phase dynamics in the absence of noise, and is referred to as dynamic tracking error. The second term represent the additional signal locking error contributed by the additive baseband noise.

The closed loop transfer function H(s) is readily expressed in terms of the loop parameters. Thus if the filter is of the lead lag form $(\tau_1 s + 1)\ (\tau_2 s + 1)^{-1}$ the open loop transfer function is simply $(K/s) \times (\tau_1 s + 1)\ (\tau_2 s + 1)^{-1}$ where K represents the product of the gains of each component of the loop. The closed loop transfer function H(s) is then given by

$$H(s) = \frac{\tau_1 s + 1}{\frac{\tau_2}{K}\ s^2 + (\tau_1 + \frac{1}{K})\ s + 1} \tag{B-8}$$

The damping factor of the poles of H(s) is given by

$$g = \frac{1}{2}\ \frac{(1 + K\tau_1)}{\sqrt{\tau_2 K}} \tag{B-9}$$

The dynamic tracking error is obtained by evaluating the inverse transform of the first term in Eq. (B-7). Let the input $\phi(t) = \mathcal{L}^{-1}\ \psi_{in}(s)$ be given by a power

$$\phi(t) = \phi(0) + \alpha t + \beta(t^2/2) + \gamma(t^3/6) \tag{B-10}$$

then

$$\phi_e(t) = \mathcal{L}^{-1}\left[1 - H(s)\right]\psi_s(s) = \left[\frac{\alpha}{K} + \frac{\beta}{\omega_n^2} - \frac{\gamma(K\tau_1+2)}{K\omega_n^2}\right] + \left[\frac{\beta}{K} + \frac{\gamma}{\omega_n^2}\right]t + \left(\frac{\gamma}{K}\right)\left(\frac{t^2}{2}\right) + \text{transients} \qquad \text{(B-11)}$$

where $\omega_n^2 = K/\tau_2$ and a small approximation has been made on the assumption that $\tau_2 >> \tau_1$ and that $K >> 1$. The transients die out within a short time interval on the order of the reciprocal of the loop bandwidth. In most applications the transients may usually be neglected.

The noise induced error is obtained by operating with the second term in Eq. (B-7). The rms value is given by

$$\phi_n(\text{rms}) = \left[\int_{-\infty}^{\infty} \left|\frac{x_q(\omega)}{E_s} \cdot H(j\omega)\right|^2 d\omega\right]^{1/2} \text{ radians} \qquad \text{(B-12)}$$

which for the case of a flat spectrum for the noise process having density, Φ is simplified to

$$\phi_n(\text{rms}) = \left(\frac{\Phi B_n}{E_s^2}\right)^{1/2} = \left(\frac{2S}{N}\right)^{-1/2}\Big|_{B_n} \text{ radians} \qquad \text{(B-13)}$$

where $S = E_s^2/2$ is the signal power, the $N = \Phi B_n$ is the noise power within the loop bandwidth and B_n, defined below, is the noise bandwidth of the loop.

In the literature B_n is defined alternatively by either the single or double sided noise bandwidth. Thus in formulations involving the noise bandwidth, a factor of two is present when the single sided noise bandwidth is used. The single sided noise bandwidth B_n is given by

$$\begin{aligned} 2B_n &= \frac{1}{2\pi}\int_{-\infty}^{\infty} |H(j\omega)|^2 d\omega \\ &= \frac{K}{2}\left(\frac{1 + K\tau_1^{\,2}/\tau_2}{1 + K\tau_1}\right) \text{ Hz} \\ &\approx \frac{1}{2}\left(\frac{1}{\tau_2} + K\tau_1/\tau_2\right) \text{ Hz for } K\tau_1 >> 1 \end{aligned} \qquad \text{(B-14)}$$

The remainder of Appendix B is devoted to general considerations relevant to the design of phase-locked loops. Some of the topics considered here are optimization, signal-to-noise level, oscillator instability, and the damping factor.

General Considerations

In the steady state condition the phase-locked loop is in essence a tracking filter, i.e., a narrowband filter with a tunable center frequency. For small phase perturbations the system behaves quite linearly, and the analysis of such a system is relatively straightforward. However, the reponse of the system to large transients and severe dynamics in the input frequency and phase is not at all straightforward, and may, indeed, be nonlinear.

A complete set of solutions to the problem involves the generation of a set of output curves corresponding to a large set of dynamic input conditions; this is complicated by the fact that the PLL contains a filter whose parameters determine the acquisition and tracking performance. The problem of designing a PLL is then to specify a set of allowable input conditions, for which some sort of "optimum" filter can be determined. "Optimum" means that some property of the error, such as the error "power", is minimized. The "optimum" filter may or may not be physically realizable. As a compromise, an approximate filter is built and the response of the system with this filter is determined for the given set of input conditions.

In general, a single integration filter (resulting in a second-order loop) allows the loop to lock on to a frequency step with zero ultimate phase error, whereas a double integration filter (resulting in a third-order loop), allows tracking of a frequency ramp with zero phase error. Since perfect integrators do not exist in practice, except for those which can be constructed digitally, other filter which are good approximations are utilized. For example, one such filter that has received wide attention is the filter of Mallinckrodt, first reported in (Ref.7). The Mallinckrodt filter is an approximation to the optimum Wiener filter. It appears that the optimum Wiener filter has complex poles and is only conditionally stable. The Mallinckrodt filter, having only real poles, is a more highly damped system and consequently a more stable one. The damped loop allows a possible gain variation of 13:1 while still remaining stable. Nevertheless an AGC is required to keep the loop gain within the allowable limits for stability. Since the loop gain is proportional to the input signal amplitude, E_s.

The problem of acquisition is one of correctly identifying a changing frequency in the presence of noise as quickly as possible and within certain small allowable error limits. The purpose of an acquisition-aiding scheme is to aid the PLL in acquiring the signal faster than it could acquire it by itself. For this reason the allowable error of the acquisition scheme depends upon the maximum pull-in range of the PLL.

Using the conventional filter $(1+\tau_1 s)/(1+\tau_2 s)$, the acquisition time for a frequency offset can be found (Ref. 8). This acquisition time is considered to have two parts, the phase acquisition time t_ϕ and the frequency acquisition time t_f. The time t_ϕ is of the same order of magnitude of the response time of a single pole filter of bandwidth B_n, which has an equivalent time constant of $2/B_n$. Thus, considering 5 time constants to be sufficient,

$$t_\phi \leq \frac{10}{2B_n} \qquad \text{(B.15)}$$

The frequency acquisition time is then the time it takes for the frequency error to reduce from the initial frequency step Δf to B_n/π; this has been found to be

$$t_f \approx 33.5 \frac{\Delta f^2}{(2B_n)^3} \text{ sec} \qquad \text{(B.16)}$$

for a loop damping of 0.707. As the damping increases t_f increases. For a damping of 2.8 the constant in the above expression nearly doubles. The above approximation is true only if Δf is well within the pull-in range of the loop. The pull-in range for a second-order PLL has been found to be

$$\Delta\omega_p \doteq \frac{\tau_1}{\tau_2} K\left(\frac{2\tau_2}{\tau_1} - 1\right)^{1/2} \qquad \text{(B.17)}$$

In Figure B-4 we have plotted the frequency acquisition time of a second-order PLL versus initial frequency offset. The expression of Eq. (B.16) holds for all values of Δf if the loop filter has an ideal integration, because then the pull-in range of the PLL is infinite.

The value of the acquisition time $(t_f + t_\phi)$ is in general too large for most applications, and thus various acquisition aiding schemes are used. Such schemes generally provide a means by which the VCO is brought to the vicinity of the input frequency. Then when the loop is locked or nearly locked, the acquisition circuitry is disabled.

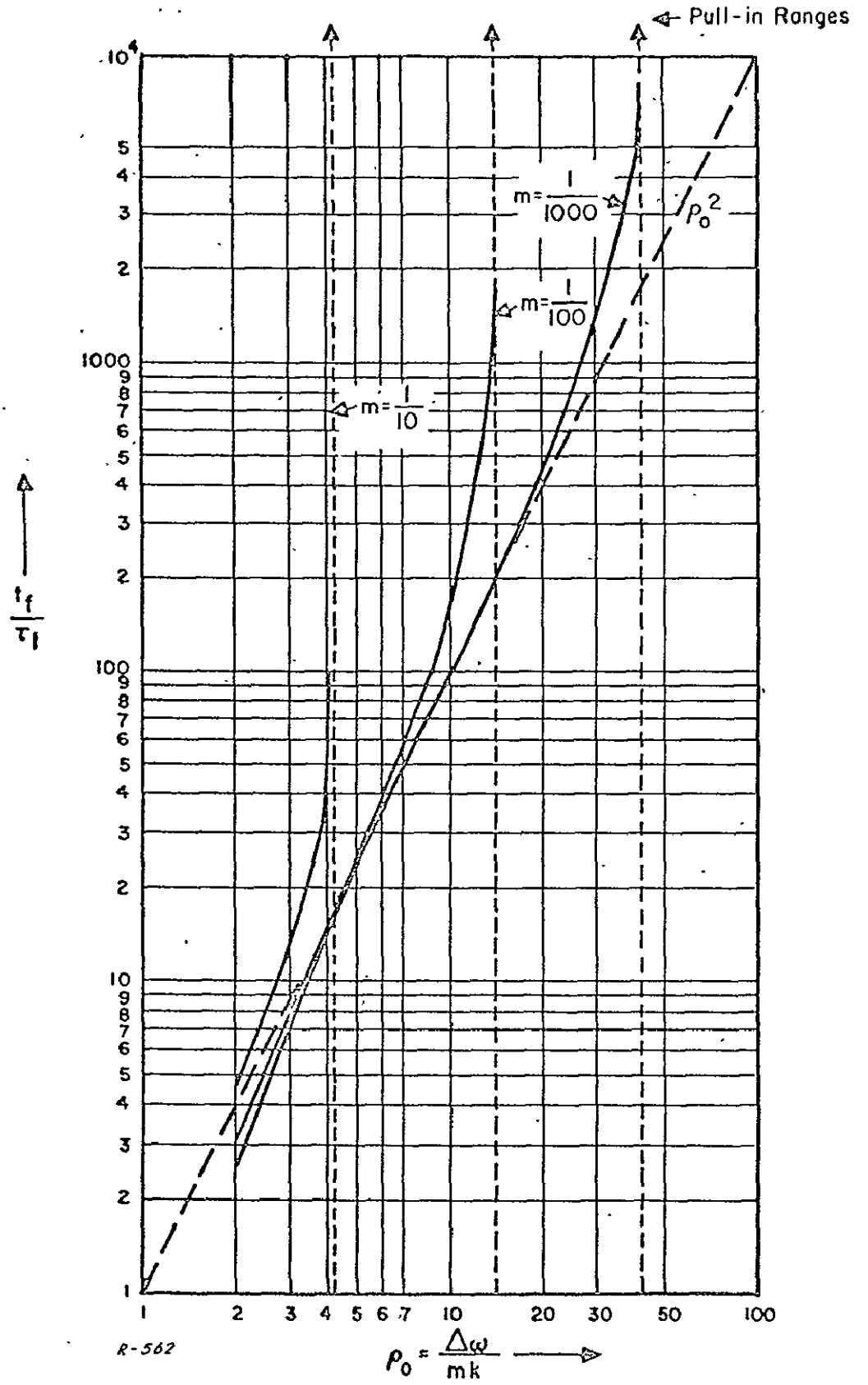

Figure B-4 Frequency Pull-in Time of a Conventional Second-Order PLL. $m = \tau_1/\tau_2$

Gain Stabilization Considerations

It will be recalled that the open loop gain K is directly proportional to the input signal level. Therefore, if the input signal varies over a wide range, then B_n and ζ also vary drastically. This variation can be reduced by the use of automatic gain control (AGC) loop. However, this results in large noise error in the loop at low signal-to-noise ratios (SNR). If variation in signal and noise levels were small, AGC would be satisfactory.

In a second-order PLL the use of an ideal limiter preceding the phase detector results in an optimum loop over a wide range of input signal and noise levels. The reason for this is that the limiter compresses the variation of the signal level into the loop. Thus at the lowest SNR the limiter suppresses the signal, and the loop noise bandwidth and damping are minimum (Ref. 9). As the signal power increases B_n and ζ increase to a constant value at strong signal levels. This saturation of B_n and ζ at strong levels occurs because the signal power at the output of the limiter saturates with increasing SNR into the limiter. Hence the loop design holds for a larger range of signal and noise levels. Obviously one disadvantage is limiter suppression of the signal at low SNR's.

Design Approach

The design of the loop for tracking proceeds by noting that the minimum damping ζ of a second-order factor should not be less than one half, and the "optimum" value of ζ from several considerations (Ref. 10) should be in the vicinity of 0.707. Since ζ increases with SNR, the minimum ζ is at minimum specified SNR. Normally the loop characteristics ζ and B_n are determined at this minimum SNR. The linearized assumption of the phase transfer model breaks down for low SNR's, and experimental results show that for SNR's below 3.2 dB (corresponding to an rms noise error in the linearized loop of about 28°) the probability of the loop staying locked is small. Thus, specifying ζ and B_n at a 0 dB SNR in the loop has been found quite meaningful. These are called the threshold values ζ_t and B_{nt}. Since the critical region of operation is at threshold, the "optimum" damping $\zeta_t = 1/\sqrt{2}$ is selected rather than the value of 1/2. Some designs may, however, use a damping of 1/2 at threshold.

The noise error of Eq. (B.13) did not include the effect of VCO noise. The VCO noise $\phi_{int}(t)$ is significant only when the loop bandwidth is narrowest. If this interval jitter can be modeled as shown in Figure B-5 when the VCO is operating in the closed loop, then the amount of phase instability produced at the VCO output is

$$\psi_o(s) = \{1 - H(s)\} \psi_{int}(s)$$

Thus the PLL acts as a high-pass filter for the VCO phase instabilities. Hence the narrower the bandwidth of H(s) the more contribution is made by VCO noise. The magnitude of $\{1 - H(j\omega)\}$ is sketched in Figure B-6 to show its high-pass behavior. The power in $\psi_{int}(s)$ can be kept small by keeping the dc gain of the loop high. Little information is available on the exact spectrum of $\psi_{int}(s)$. However, it is well established that it represents no more than a small disturbance and is a function of the required VCO deviation such that the larger the deviation, the larger is $\psi_{int}(s)$.

The above relations have shown that the noise and dynamic errors are worst at threshold. Therefore, the design approach is to satisfy the loop specifications on these errors at threshold, their satisfaction at the higher SNR's being automatically guaranteed. To determine the performance of the loop at the higher SNR's the relationship of B_n and ζ versus input SNR is obtained using the limiter curve of Davenport (Ref. 9). Assuming that the threshold damping is $\zeta_t = 0.707$, the filter time constants τ_1 and τ_2 can be expressed in terms of the specified threshold noise- bandwidth B_{nt} and the open loop gain at threshold (K_t) as

$$\tau_1 = \frac{3}{4 B_{nt}} \tag{B-18}$$

$$\tau_2 = \frac{9}{16} \frac{K_t}{B_{nt}^2} \tag{B-19}$$

With these values of τ_1 and τ_2, the noise bandwidth may be written as

$$B_n = \frac{B_{nt}}{3} \left(2 \frac{K}{K_t} + 1\right) \tag{B-20}$$

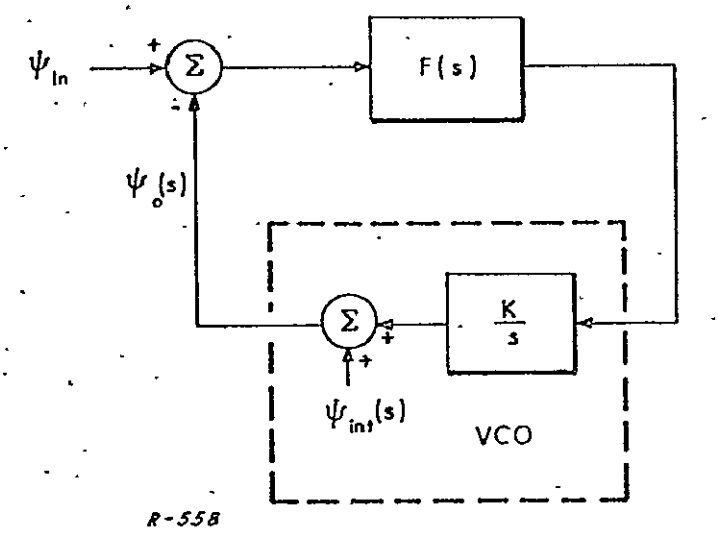

Figure B-5 PLL Phase Transfer Model: Oscillator Instability

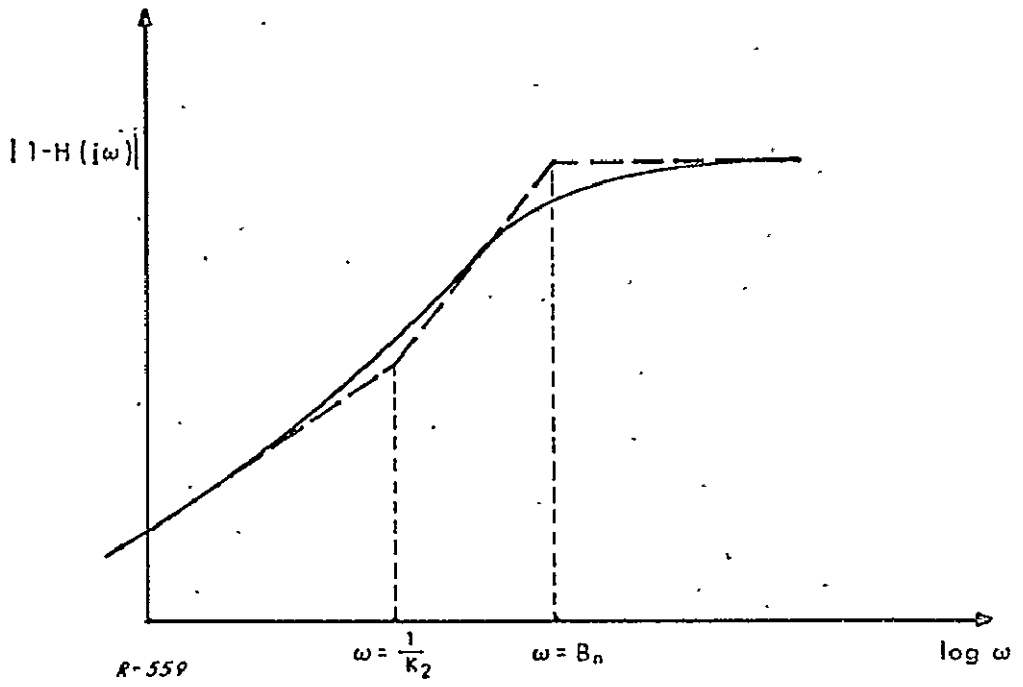

Figure B-6 Bode Plot of $\left|1 - H(s)\right|$

where K is determined from Davenport's curve. Similarly the variation in damping is

$$\zeta \approx \zeta_t \sqrt{\frac{K}{K_t}} = \sqrt{\frac{K}{2K_t}} \quad \text{since } \zeta_t = \frac{1}{\sqrt{2}} \tag{B-21}$$

In the usual case where the threshold corresponds to the weak signal limit of Davenport's limiter curve, the strong signal noise bandwidth has been found from Eq. (B. 20) to be

$$B_{ns} = \frac{B_{nt}}{3} \left(2 \sqrt{\frac{B_{i-f}}{B_{nt}}} + 1\right) \tag{B-22}$$

Thus the loop noise bandwidth varies with input SNR from B_{nt} to B_{ns}.

Appendix C

DESIGN AND PERFORMANCE OF PRACTICAL SYSTEMS

The discussion of Appendix A has given the derivation and meaning of many of the results used in classical radar design. This section presents analyses of commonly used ranging tracker techniques. The noise and dynamic performance obtainable from these practical techniques are determined and compared to those obtainable from optimum implementations.

Split Gate Tracker

The split gate tracker is well known for its use in range tracking equipment. It obtains near optimum ranging accuracy from the input pulse train signal. It is readily analyzed in terms of a linear model which is similar to that of the phase-locked loop. The linearized model is developed below and performance analyses based on this model are given.

System configuration and linearized model. -- A simple split-gate tracking loop is shown in Figure C-1.

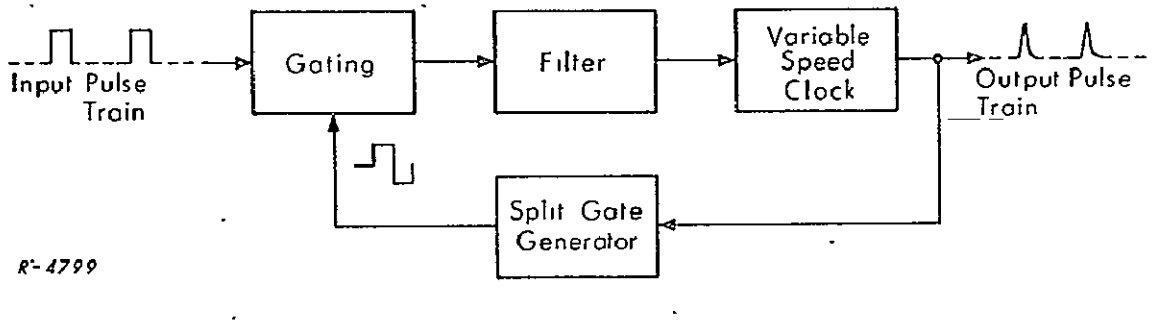

Figure C-1 Simple Split Gate Tracking Loop

The loop accepts the input pulse train and produces an output pulse train which is locked to the input. The loop acts as a smoothing filter which substantially reduces the noise content of the pulse train by reducing the noise bandwidth of the system.

The output pulse train is locked to the input in the following way. Each output pulse triggers the generator to produce a split gate. The split gate combines with the input pulse in the gating unit to produce an error signal which indicates whether the output is leading or lagging the input. The error signal is also in the form of a pulse train. It is smoothed in the filter and then used to control the clock speed to bring the output into coincidence with the input.

The error signal is obtained as follows. The split gate contains both a positive and a negative region. These are sometimes called the "early" and "late" gates. The gating unit functions as a multiplier which multiplies the positive input pulse by the split gate waveform. Thus the output of the gating unit is a pulse waveform containing both positive and negative regions which are equal only when the loop output is in coincidence with the loop input. The difference between the positive and negative regions is the value of the error signal.

The filter acts as an integrator which combines the positive and negative regions of the error waveform to give a voltage level which is equal to the difference between the positive and negative areas. This voltage level serves as the control signal for the variable speed clock.

A simple range tracker employing a split gate tracking loop is shown in Figure C-2. The figure represents one of a number of possible configurations for a tracking filter. The variable speed clock is shown in greater detail; it consists of a voltage controlled oscillator (VCO), a cycle counter and a comparator. Each time the counter reaches a preset number, N, the comparator generates a pulse to trigger the split gate generator. A similar arrangement is employed to generate the "Main Bang" trigger which initiates the transmission of the signal to the target. The difference between the contents of the counters results from the delay in propagation of the signal to the target and back to the receiver. Thus, the difference, with a suitable scale factor, represents the range.

The linearized model is developed with aid of Figure C-3. Here the split gate tracker has been redrawn so that the VCO appears separately from the counter and split gate generator which have been combined in a single unit. Also the gating unit is shown as a multiplier. The input and output (split gate) waveforms are shown respectively by $f(t + t_i)$ and $g(t + t_o)$. The argument of the input time function is $t + t_i$ rather than simply t in order to point out later the similarity between the split gate tracker and the phase-locked loop. The term t_i may be thought of as a time delay modulation in the signal propagation time such as would be experienced by an altimeter when the altitude is not constant.

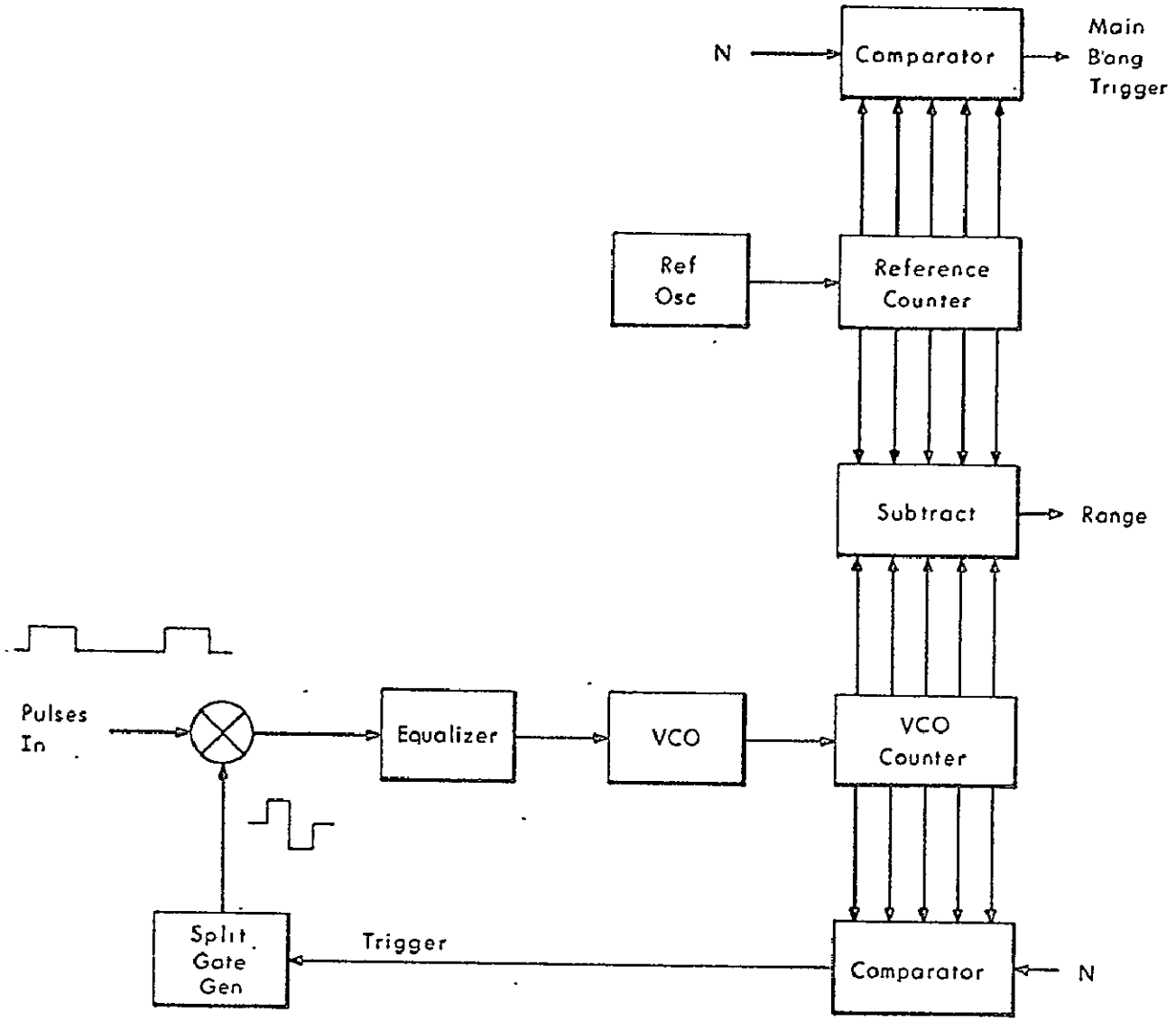

Figure C-2 An All Electronic Range Tracker

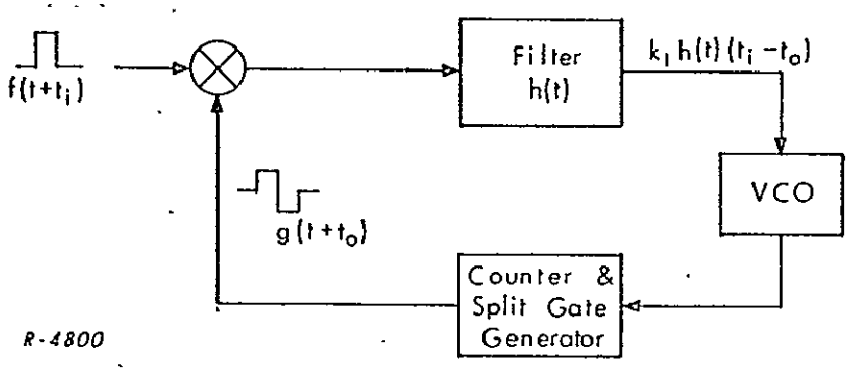

Figure C-3 Time Signals In Split Gate Loop

Similarly t_o may be regarded as the time delay modulation at the loop output.

The output of the filter in Figure C-3 is shown as $k_1 h(t)\ (t_i - t_o)$, where k_1 is a constant defined below and h(t) is the impulse response of the filter. The output is related to the input as follows. The input to the filter is of short duration compared to h(t) and may therefore be regarded as an impulse whose value is equal to the area of the positive portion minus the area of the negative portion, without affecting the validity of the expression for the filter output. The value of the impulse is a function of $(t_i - t_o)$ as is shown in Figure C-4. For small values of $(t_i - t_o)$ the value of the impulse varies linearly with the slope of the curve given by k_1. Thus the filter output is given by

$$h(t) \otimes [k_1 (t_i - t_o)\ u_o(t)] = k_1 h(t)\ (t_i - t_o)$$

The filter also serves as the connecting link between the split gate tracker and the phase-locked loop. It provides for the same type of operation in both loops even though one loop accepts a continuous wave. The filter can effect the similarity in operation when its bandwidth is very much smaller than the pulse repetition frequency (PRF). Under this condition the contributions of the pulses in the input pulse train are effectively summed together to form a continuous output from the filter. The continuous output of the filter in the case of the split gate tracker is virtually indistinguishable from that of the phase-locked loop. Note further, that poisson noise spikes at the input to the filter will result in approximately Gaussian noise at the output of the filter.

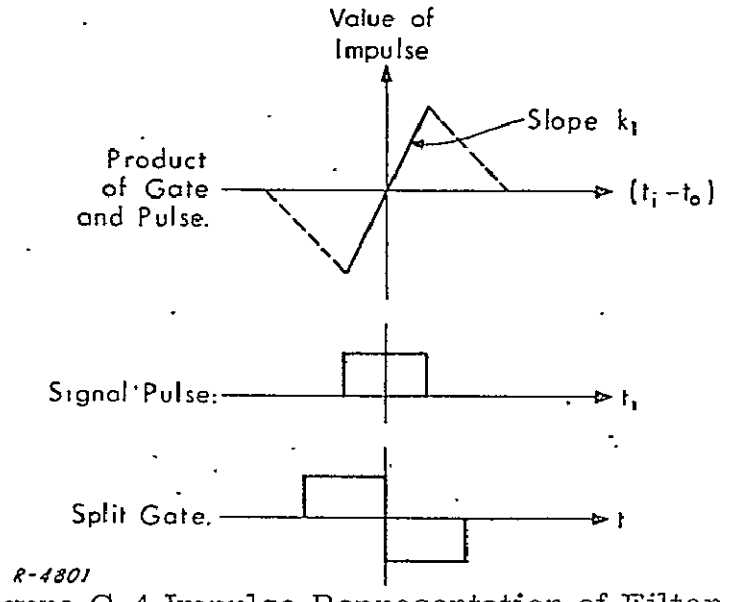

Figure C-4 Impulse Representation of Filter Input

A further simplification can now be made in the notation. Since the loop response is a function only of $(t_i - t_o)$, the term t may be dropped from the expressions for the input and output waveforms. This is equivalent to viewing these signals in a moving coordinate system, t merely defines an arbitrary reference phase for the system.

The configuration of Figure C-3 may now be recast to show the Laplace transform representation shown in Figure C-5. The purpose of this representation is to predict the time lag between the loop input and output. The time lag may be related to the phase of the PRF, thus, this representation is often referred to as a phase model. The functions f and g may therefore be dropped and the input and output signals are represented as the Laplace transforms of the input and output time modulations. The counter and split gate generator have been deleted since they are of much wider bandwidth than the loop bandwidth and may therefore be regarded as frequency independent. The VCO is shown by the usual representation as an integrator since its output phase is the integral of its frequency which is, in turn, proportional to the control voltage provided by the filter. This representation of the VCO is valid for the split gate tracking loop since the phase of the VCO output is linearly related to the time lag between the loop input and loop output. The constant K includes k_1 as well as all other gains that may be present such as those of the operational amplifier (not shown) used to drive the VCO, the VCO gain itself, and the attenuation (phase division) of the counter.

The representation of Figure C-5 is identical to that of a phase-locked loop. All analyses applicable to phase-locked loops are thus applicable to the split gate tracking loop within the linear regions of both loops. The two loops differ in their acquisition performance since the split gate tracker requires a strobing action to located the input pulse. In addition, the noise transfer characteristic through the split gate requires a more complicated analysis than that used for the PLL input mixer.

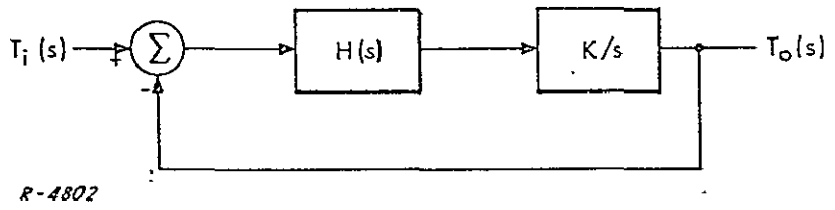

Figure C-5 Transform Representation of Split Gate Loop

The open loop transfer function for the case where a lead lag filter is employed is given by $(K/s)(\tau_1 s + 1)(\tau_2 s + 1)^{-1}$. Increased performance can be obtained by using a lead filter followed by an additional integrator. Such an integrator can be built by digital techniques. The resulting open loop transfer function is then given by $(K/s^2)(\tau_1 s + 1)$.

For purposes of analysis the split gate tracking loop is generally treated as a filter with input $T_i(s)$ and output $T_o(s)$. The transfer function of this filter is simply the closed loop transfer function of the split gate loop. In the case of the lead lag filter and single integration it is given by Eq. (B-8) which is recase for convenience as

$$H_L(s) = \omega_n^2 \frac{\tau_1 s + 1}{s^2 + 2\zeta\omega_n s + \omega_n^2} \qquad (C-1)$$

where $\omega_n^2 = K/\tau_2$ amd $2\zeta = \omega_n(\tau_1 + K^{-1})$. In the case of the lead filter and double integration it is given by Eq. (C-1) with $\omega_n^2 = K$ and $2\zeta = \omega_n\tau_1$. The exact form of the closed loop response of the tracker determines its dynamic performance and is an important factor in determining its noise performance. These details are discussed below.

One further comment is in order, namely, the reason for selecting a split gate rather than some other form of gate. The optimum form of gate is give by the derivative of the signal waveform (Ref.11). In a practical range tracker, the tracking loop is preceded by an IF amplifier and filter which distorts a square pulse so that it acquires a trapezoidal or triangular envelope. Near optimum IF filtering is fairly narrow to exclude as much noise as possible without seriously affecting the pulse. The output pulse envelope for such filtering resenbles the matched filter output, i.e., a triangle. The derivative of a triangle is the split gate waveform. By way of comparison with the phase-locked loop the same relationship exists, e.g., the gating waveform, a cosinusoid, is the derivative of the input signal waveform, a sinusoid. In the following section the optimum relationship between IF filter bandwidth and gate width is developed for a specific pulse width.

Noise error.-- This section treats a practical system containing the split gate tracking loop preceded by an IF amplifier and a detection circuit which demodulates the IF carrier to give the pulse envelope waveform. The input signal to the IF amplifier is accompanied by noise, some of which passes through the amplifier to induce a noise error at the output of the split gate tracking loop. The noise error manifests

itself in the form of a jitter on the output pulse train. In this section the magnitude of the noise error is investigated and the noise transfer characteristic of the split gate is derived.

The following parameters play a key role in the evaluation of the noise error, namely, the bandpass characteristic of the IF amplifier, the average power and duty factor of the input pulse train, the width of the split gate, and the noise bandwidth of the split gate loop where the loop is treated as a filter. It is shown below that for a given pulse width, there is a relationship between the IF filtering and the width of the split gate which maximizes the effective SNR presented to the split gate tracker. The amount of noise passed by the split gate is further reduced by the noise bandwidth of the loop. And finally, the noise is also reduced by the gating action itself since the split gate gates out all noise except that which is present at the instant when a pulse is received.

The analysis proceeds as follows. First the noise voltage and the signal pulse waveform outputs of the IF filter are calculated for a simple filter shape. Then the error voltage generated by multiplying the resulting pulse waveform with the split gate waveform is obtained as a function of timing error. This is equated with the noise voltage to determine the split gate timing error associated with a given signal and noise level. The timing error is then minimized by determining the best relationship between the IF filter parameter and the width of the split gate for a given pulse width.

At this point all parameters of the system have been specified except for the gain and bandpass characteristics of the split gate tracking filter. A typical tracking filter is assumed for the remaining calculations which give the noise error at the output of the split gate tracker.

To begin the calculations, an IF filter is selected whose bandpass characteristic is equivalent to a double RC rolloff at baseband. For the purposes of this analysis it suffices to consider only the baseband representation. The lowpass filter transfer function is given by

$$H_{LP}(s) = \left(\frac{a}{s + a}\right)^2 \qquad \text{(C-2)}$$

where $1/a = RC$, the time constant. This filter and the split gate are shown in Figure C-6.

The noise admitted by the split gate is found as follows. The input and output noise voltage waveforms of the lowpass filter are represented by n(t) and m(t) respectively. The split gate voltage waveform is represented by g(t). τ_g is the gate width and the two sections of the

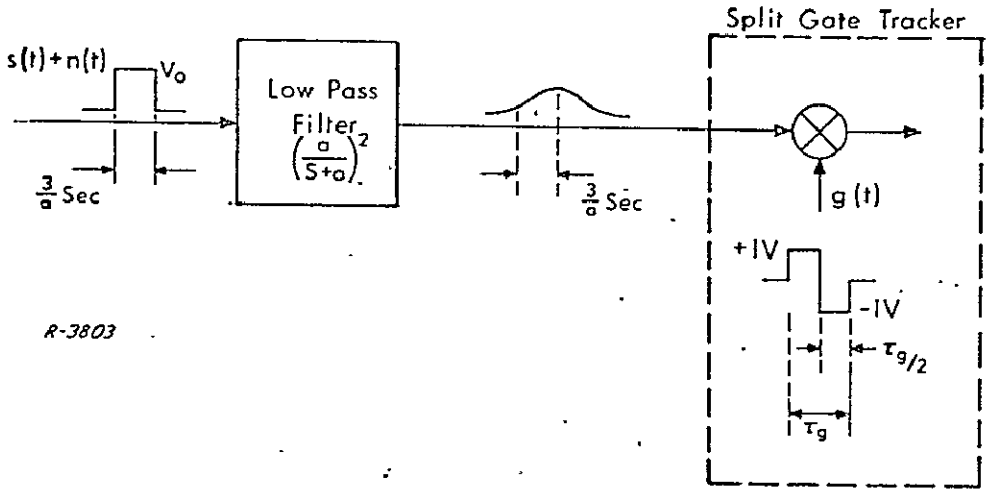

Figure C-6 Video Input To Split Gate

gate have equal durations of $\tau_g/2$. g(t) is given by

$$g(t) = \begin{cases} 0; & t < -\tau_{g/2},\ t \geq +\tau_{g/2} \\ +1; & -\tau_{g/2} \leq t < 0 \\ -1; & 0 \leq t < \tau_{g/2} \end{cases} \qquad \text{(C-3)}$$

In a practical system g(t) occurs periodically but for the purposes of this part of the analysis it is assumed that g(t) occurs only once. The integral of the noise voltage passed by the split gate is given by

$$e_n = \int_{-\infty}^{\infty} m(t)\, g(t)\, dt \qquad \text{(C-4)}$$

The mean square value is given by

$$\overline{e_n^2} = \int_{-\infty}^{\infty} \int_{-\infty}^{\infty} \overline{m(t_1)\, m(t_2)}\, g(t_1)\, g(t_2)\, dt_1\, dt_2 \qquad \text{(C-5)}$$

where the bar indicates an average value.

The mean square value is readily expressed in terms of the autocorrelation functions of the noise and gate waveforms, namely, $R_m(\tau)$ and $R_g(\tau)$. Since the noise is wide sense stationary,

$$R_m(t_1 - t_2) = \overline{m(t_1)\, m(t_2)} \qquad \text{(C-6)}$$

Substituting Eq. (C-6) into Eq. (C-5) gives

$$\overline{e_n^2} = \int_{-\infty}^{\infty} \int_{-\infty}^{\infty} R_m(t_1 - t_2)\, g(t_1)\, g(t_2)\, dt_1\, dt_2 \qquad \text{(C-7)}$$

With a change of variables, $t_1 - t_2 = \tau$, this becomes

$$\overline{e_n^2} = \int_{-\infty}^{\infty} \int_{-\infty}^{\infty} R_m(\tau)\, g(\tau + t_2)\, g(t_2)\, dt_2\, d\tau \qquad \text{(C-8)}$$

Integration with respect to t_2 gives

$$\overline{e_n^2} = \int_{-\infty}^{\infty} R_m(\tau)\, R_g(\tau)\, d\tau \qquad \text{(C-9)}$$

which is the desired expression for the mean square value of the noise voltage in terms of the autocorrelation functions, $R_m(\tau)$ and $R_g(\tau)$.

$R_g(\tau)$ is readily found by inspection; it is shown in Figure C-7.

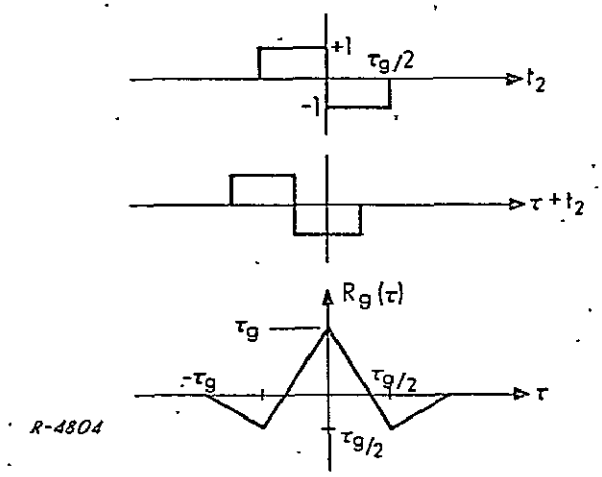

Figure C-7 Split Gate Correlation Function

$R_m(\tau)$ is found by taking the inverse transform of the power spectral density function of the noise, $S_m(\omega)$, by evaluating residues for poles in the left half plane only, and then applying the fact that $R_m(\tau)$ is symmetric in τ. $S_m(\omega)$ is given by

$$S_m(\omega) = N_o |H_{LP}(\omega)|^2 = N_o \left(\frac{a^2}{\omega^2 + a^2} \right)^2 \qquad \text{(C-10)}$$

where N_o is the noise power spectral density. The inverse transform is given by

$$R_m(\tau) = \frac{1}{2\pi j} \int_{c-j\infty}^{c+j\infty} S_m(s)\, e^{s\tau} ds = \sum_{j=1}^{n} \frac{1}{(m-1)!} \frac{d^{m-1}}{d_s^{m-1}} (s-s_j)^m S_m(s) e^{s\tau} \Big|_{s=s_j} \tag{C-11}$$

where m is the order of a pole s_j. Factoring $S_m(\omega)$ gives $N_o a^4 (j\omega+a)^{-2} (j\omega-a)^{-2}$. To take the inverse transform of $S_m(\omega)$, substitute s for $j\omega$. Then Eq. (C-11) may be solved for residues in the left half plane giving

$$R_m(\tau)\big|_{\tau>0} = \frac{1}{1!} \frac{d}{ds} \left[\frac{(s+a)^2 N_o a^4}{(s+a)^2 (s-a)^2} e^{s\tau} \right]_{s=-a} = \frac{N_o a}{4} e^{-a\tau} (1+a\tau) \tag{C-12}$$

The value of the noise voltage given by Eq. (C-9) may now be expressed directly in terms of the system parameters for $R_g(\tau)$ as given by Figure C-7 and $R_m(\tau)$ as given by Eq. (C-12). Thus

$$\overline{e_n^2} = \frac{N_o a \tau_g}{2} \left[\int_0^{\tau_g/2} \left(1 - \frac{3\tau}{\tau_g}\right) (1+a\tau) e^{-a\tau} d\tau - \int_{\tau_g/2}^{\tau_g} \left(1 - \frac{\tau}{\tau_g}\right) (1+a\tau) e^{-a\tau} d\tau \right] \tag{C-13}$$

Evaluating the integrals gives

$$\overline{e_n^2} = \frac{N_o \tau_g}{2} \left[2 + 2e^{-a\tau_g/2} + \frac{12}{a\tau_g} e^{-a\tau_g/2} - \frac{9}{a\tau_g} - e^{-a\tau} - \frac{3}{a\tau_g} e^{-a\tau_g} \right] \tag{C-14}$$

$$= (N_o \tau_g / 2)\, f_1(a\tau_g)$$

where the function $f_1(a\tau g)$ has been introduced to simplify the notation. Figure C-8 shows a plot of $f_1(a\tau g)$ as a function of $a\tau g$.

In summary $\overline{e_n^2}$ is the mean square response of the lowpass filter plus the gate to white noise of density N_o.

The next step in the analysis is to calculate the response of the lowpass filter $H_{LP}(s) = a^2/(a+s)^2$ to a pulse. For convenience, let the pulse amplitude be given by V_o and the width, τ_p, by $3/a$. The pulse

P(t), may be expressed as a positive going step plus a negative going step which has been delayed by $\tau_p = 3/a$ seconds. Thus

$$P(t) = V_o \left[u_{-1}(t) - u_{-1}(t-\tau_p) \right] \tag{C-15}$$

The response of the lowpass filter to the pulse is given by

$$f_{p1}(t) = V_o \Big[(1 - e^{-at} - a t e^{-at})\, u_{-1}(t) - \Big((1 - e^{-a(t-\tau_p)} - a(t-\tau_p) e^{-a(t-\tau_p)} \Big)\, u_{-1}(t-\tau_p) \Big] \tag{C-16}$$

The pulse response for $\tau_p = 3/a$ is plotted in Figure C-9. In order to facilitate calculations, the actual pulse is approximated by a raised cosine $f_p(t)$ which is also plotted in Figure C-9 for purposes of comparison. It is assumed, for convenience of analysis that

$$f_p(t) \cong 0.4\, V_o \left(1 + \cos \frac{\pi a}{3.5} t\right) \tag{C-17}$$

At this point the response of the gate to the filtered pulse, $f_p(t)$, is found for the case when the gate is slightly offset from the center of the pulse. This situation is illustrated in Figure C-10. The response is obtained by multiplying the pulse waveform by the gate and integrating the product over the width of the gate. This gives the error voltage e_e,

$$e_e = 0.4\, V_o \left[\int_{-\tau_g/2 + \Delta t}^{\Delta t} \left(1 + \cos \frac{\pi a}{3.5} t\right) dt - \int_{\Delta t}^{\Delta t + \tau_g/2} \left(1 + \cos \frac{\pi a}{3.5} t\right) dt \right] \tag{C-18}$$

Evaluating the integrals gives

$$e_e = 0.4\, V_o \left[\frac{7}{\pi a} \sin \frac{\pi a \Delta t}{3.5} \cdot 2 \sin^2 \frac{\pi a \tau_g}{14} \right] \tag{C-19}$$

For small error in time, Δt, this can be approximated by

$$e_e \cong 0.4\, V_o \frac{7}{\pi a} \frac{\pi a}{3.5} \Delta t \cdot 2 \sin^2 \frac{\pi a \tau_g}{14} \simeq 1.6\, V_o \Delta t f_2(a\tau_g) \tag{C-20}$$

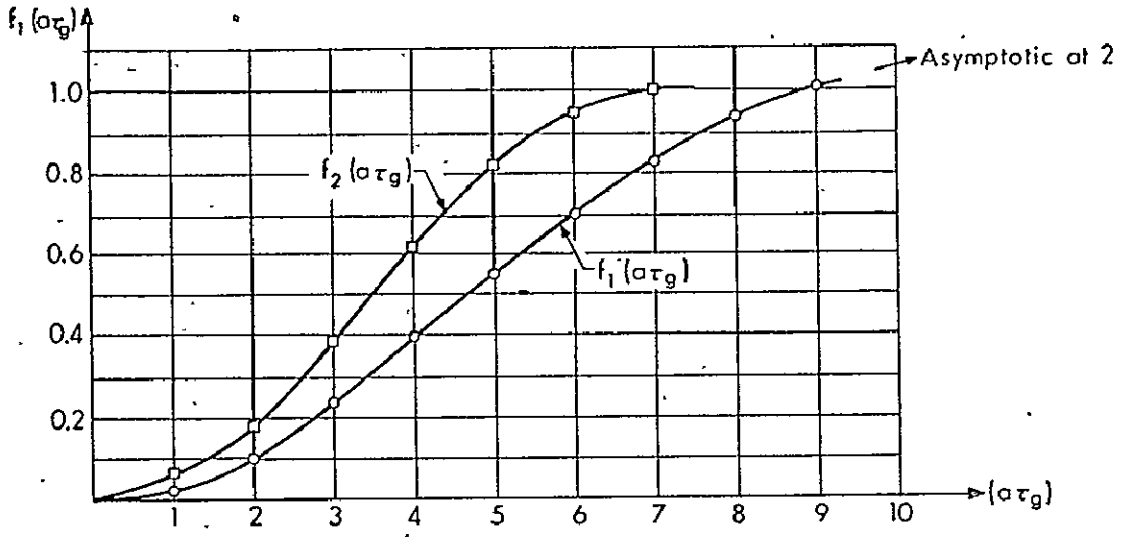

Figure C-8 Plot of $f_1(a\tau_g)$ and $f_2(a\tau_g)$

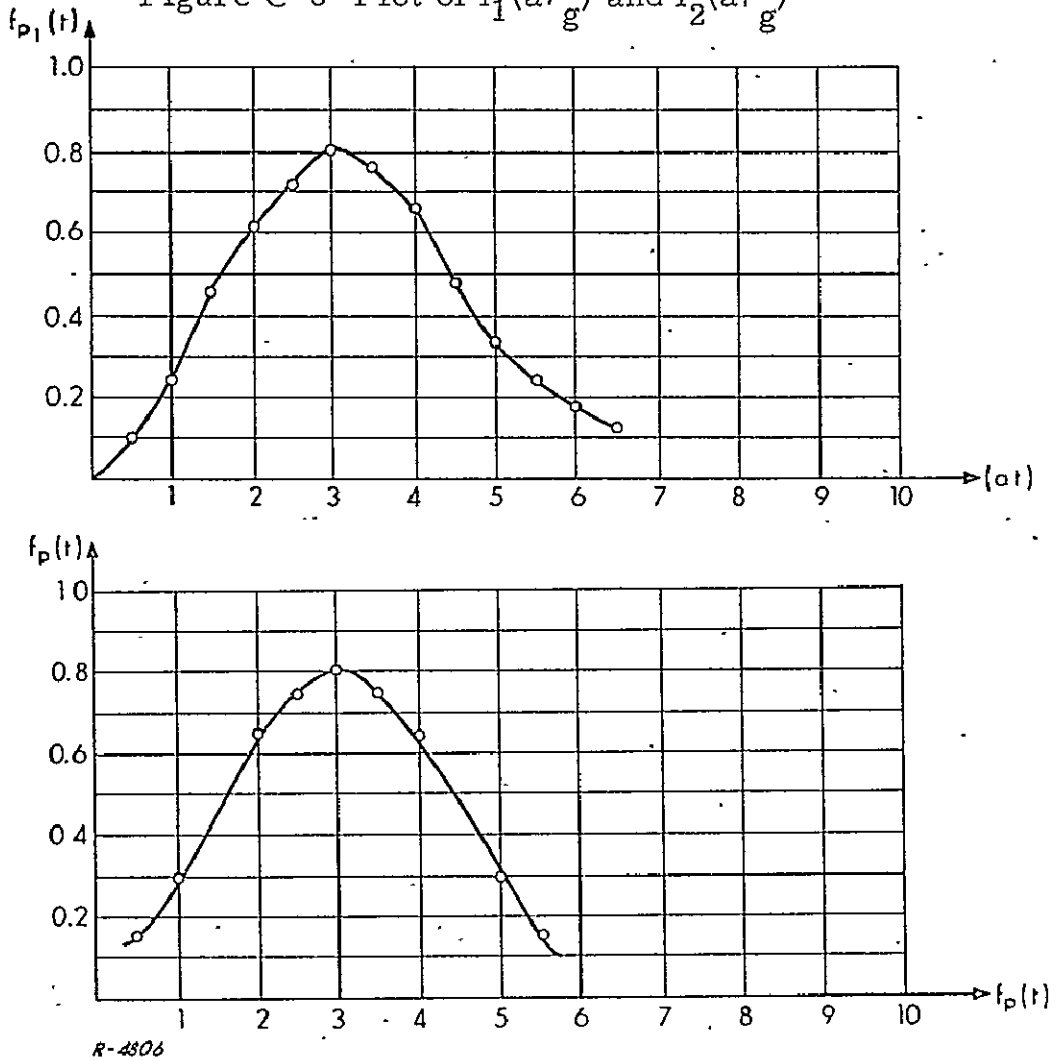

Note: Curves are given by Eqs. (C-16) and (C-17)

Figure C-9 $f_{p_1}(t)$ and its Approximation $f_p(t)$

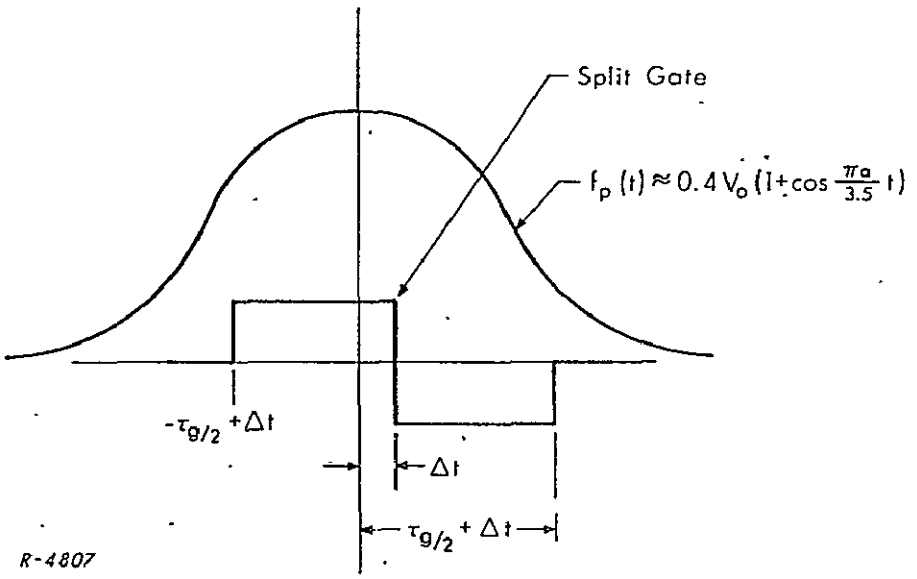

Figure C-10 Gate and Pulse Positions for Calculation of Error Response

where the notation has been simplified by the introduction of $f_2(a\tau_g)$. For convenience $f_2(a\tau_g)$ is plotted with $f_1(a\tau_g)$ in Figure C-8.

In the derivation above it was assumed that the gate was displaced causing an output error voltage e_e. However, the reverse can also happen. That is, a perturbing voltage $e_n = e_e$ will cause the gate to be displaced by an amount Δt. Thus, the relationship between rms noise and rms time error is established by equating the expression for e_e Eq. (C-20) with e_n, Eq. (C-14). Also Δt is replaced by the rms timing error σ_t giving

$$\sigma_t = \frac{\sqrt{\overline{e_n^2}}}{1.6\, V_o f_2(a\tau_g)} \tag{C-21}$$

Substituting for $\overline{e_n^2}$, from Eq. (C-14), gives

$$\sigma_t \frac{\tau_g^{1/2} f_1^{1/2}(a\tau_g)}{(1.414)(1.6)(V_o/\sqrt{N_o}) f_2(a\tau_g)} \tag{C-22}$$

The rms timing error, σ_t, can be expressed in terms of the fundamental quantities E_o, the pulse energy and N_o. The rf pulse energy is given by

$$E_o = (V_o^2/2)\tau_p = (V_o^2/2)\,(3/a) \tag{C-23}$$

Recasting gives

$$V_o = \sqrt{\frac{2E_o a}{3}} \tag{C-24}$$

Finally, σ_t can be expressed in terms of R the ratio of signal energy to noise power per cps by substituting Eq. (C. 24) into Eq.(C. 22) giving

$$\sigma_t = \frac{1}{(1.31)a\sqrt{R}\left[\dfrac{f_2(a,\tau_g)}{(a\tau_g f_1(a\tau_g))^{1/2}}\right]} \tag{C-25}$$

where R is the signal energy-to-noise power per Hz, $2E/N_o$.

Figure C-11 shows a graph of the ratio $f_2(at)/(a\tau_g f_1(a\tau_g))^{1/2}$ vs $a\tau_g$. The optimum value occurs at $a\tau_g \cong 4.5$. The minimum tracking error obtained with this system is

$$\sigma_{t_{min}} \cong \frac{1}{0.64\, a\sqrt{R}} \tag{C-26}$$

The above result can be compared with the optimum range detectibility of Woodward (Ref. 3) which is

$$\sigma_t = \frac{1}{\beta\sqrt{R}} \tag{C-27}$$

The rms bandwidth, β, of a rectangular pulse is infinite. However, under the condition that (receiver bandwidth) x (pulse duration) is greater than unity, the rms bandwidth is approximated by (Ref.12)

$$\beta \cong \sqrt{\frac{2BW}{\tau_p}} \qquad (BW)(\tau_p) \geq 1 \tag{C-28}$$

The lowpass filter considered here has single-sided bandwidth = 0.65a. The rms bandwidth is

$$\beta \cong \sqrt{\frac{1.3a}{3/a}} = 0.658a \tag{C-29}$$

The range accuracy of the optimum receiver is then,

$$\sigma_{\tau_{opt}} = \frac{1}{0.658a\sqrt{R}} \tag{C-30}$$

The best range accuracy obtainable from the receiver under consideration is less than optimum by a factor of $(0.658/0.64) \approx 1.02$ or about 2%. This result agrees with the obtained by Barton (Ref.13) for the split gate tracker, which is

$$\sigma_{t_{opt}} = \frac{\tau_p}{2\sqrt{R}} \tag{C-31}$$

or, for $\tau_p = 3/a$

$$\sigma_{\tau_{opt}} = \frac{1}{0.67a\sqrt{R}} \tag{C-32}$$

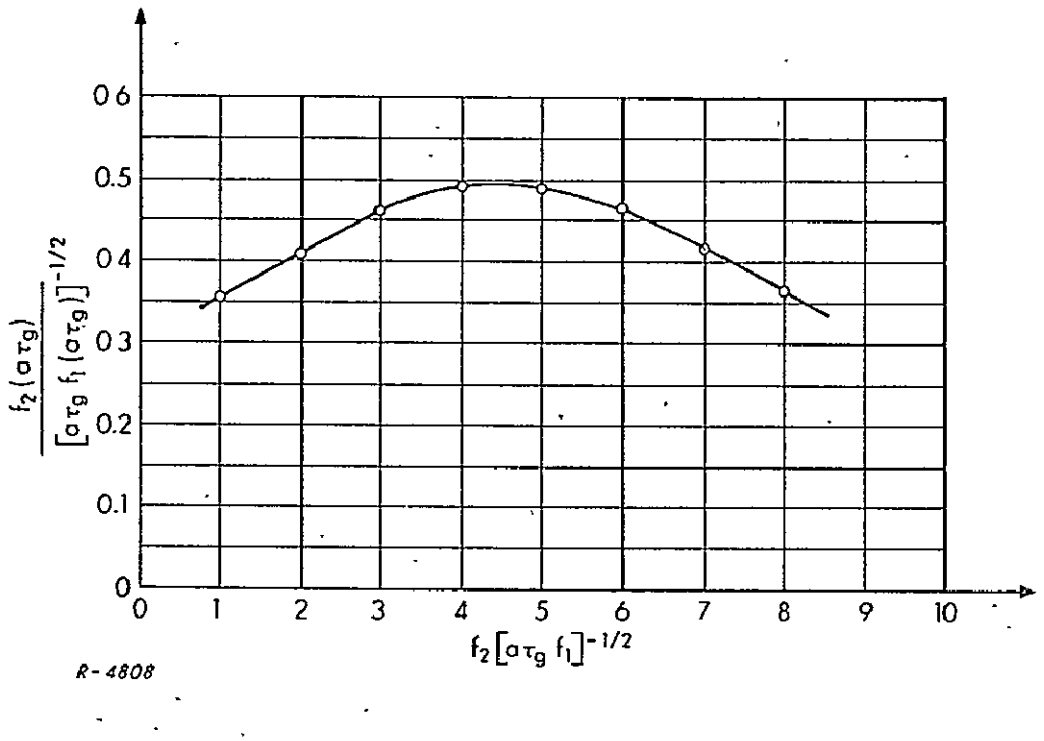

Figure C-11 Plot of Ratio, a Function of f_1 and f_2

Effect of the split gate loop.-- So far, the analysis of the noise error has considered only the equivalent lowpass filter representation of the IF filter and the split gate. At this point the complete split gate tracking loop is considered. Since it acts as a filter, it can further reduce the noise error if the loop noise bandwidth is less than the bandwidth of the noise at the split gate, or equivalently, if the loop noise bandwidth is less than that of the lowpass filter. This condition is fulfilled in practical systems, so that there is a substantial reduction in the noise induced error.

The effect of the split gate loop may be analyzed by comparing the IF spectrum with the baseband spectrum following the procedure of Barton (Ref.13). The input signal at IF is a periodic pulse signal with a line spectrum. The spectral line separation equals f_r, the pulse repetition frequency. The total noise N passed by the IF bandwidth, B_{if} is $N = N_o' B_{if}$ where N_o' is the average value of the noise spectral density at IF. At baseband this spectrum is folded over and filtered by the split gate loop. The action of this filtering on the noise is readily seen by superimposing the loop noise bandwidth, B_n (single sided) on the IF spectrum. The only noise contributing to the noise error is that contained within regions of $2B_n$ centered at each spectral line. Since there are (B_{if}/f_r) spectral lines, the total noise is given by $N_o' (2B_n)(B_{if}/f_r) = N(2B_n/f_r)$. Thus the effect of the loop filtering is to reduce the average noise power by a factor of $(2B_n/f_r)$.

This result may be applied to the noise induced error σ_t given by Eq. (C-26). First it is noted that $R = 2E/N_o$ is proportional to the SNR, the ratio of the average signal power within the split gate to the average noise power within the gate. Therefore the improvement factor, $(2B_n/f_r)$, may be applied directly giving

$$\sigma_t = \frac{1}{0.64a\sqrt{(R)(f_r/2B_n)}} = \frac{1}{0.64\sqrt{\frac{S_{ave}}{N_o B_n}}} \qquad \text{(C-33)}$$

where $S_{ave} = E \cdot f_r$ is the average signal power. In this expression B_n is given by

$$2B_n = \frac{1}{2\pi j}\int_{-\infty}^{\infty} |H_L(s)|^2 \, ds \qquad \text{(C-34)}$$

where $H_L(s)$, the split gate loop transfer function, is given by Eq. (C-1).

The improvement in the precision as shown by Eq. (C-33) is to be expected. The loop, acting as a filter, sums the results from a large number of pulses to produce each output data sample. The output data rate is given approximately by $2B_n$ as is indicated by the sampling theorem, $2TW = 1$, where T is the sample time and W is the filter bandwidth. Since $f_r >> 2B_n$ it is clear that each output sample is the average of a large number of input data pulses.

Dynamic error. -- The dynamic tracking error is a function of both the IF filtering and the split gate tracking loop bandpass characteristic. In a typical system the IF bandwidth is very much wider than the tracking loop bandwidth and therefore has a negligibly small effect on the system dynamic performance. Under this condition the dynamic performance is determined by the tracking loop bandpass characteristics.

The dynamic response is based on the representation of Figure C-5 in order to permit the well known formulations of the phase-locked loop to be applied directly to the split gate tracker loop. The dynamic tracking error $T_e(t)$ is given by

$$T_e(t) = T_i(t) - T_o(t) = \mathcal{L}^{-1}\left\{T_i(s)\left[1-H_L(s)\right]\right\} \qquad \text{(C-35)}$$

where $H_L(s)$ is given by Eq. (C-1). Let the input be represented by a power series of the same form as that given in Eq. (B-10).

$$T_i(t) = T_i(o) + \dot{\alpha}t + \beta\left(\frac{t^2}{2}\right) + \gamma\left(\frac{t^3}{6}\right) \qquad \text{(C-36)}$$

For a split gate loop containing a lead lag filter and a single integration, the tracking error in response to the input power series is the same as that given in Appendix B; it is repeated for convenience.

$$T_e(t) = \left[\frac{\alpha}{K} + \frac{\beta}{\omega_n^2} - \frac{\gamma(K\tau_1+4)}{K\omega_n^2}\right] + \left[\frac{\beta}{K} + \frac{\gamma}{\omega_n^2}\right]t + \left(\frac{\gamma}{K}\right)\left(\frac{t^2}{2}\right) + \text{transients} \qquad \text{(C-37)}$$

in which a small approximation has been made on the assumption that $\tau_2 >> \tau_1$, and $K>>1$. The transients die out within a short time interval on the order of the reciprocal of the loop bandwidth. In most applications they can usually be neglected.

For a split gate tracking loop containing a lead filter and a double integration, the steady state tracking error in response to the input power series is given by

$$T_e(t) = \left[\frac{\beta}{K} - \frac{\gamma\tau_1}{K}\right] + \frac{\gamma}{K}\, t \qquad \text{(C-38)}$$

which shows that a double integration reduces the powers of t in the expression for the dynamic error.

These results might indicated that a system employing a third ideal integrator would provide improved performance. Each integration simply removes the effect of one more term in the power series representation of the input signal. But the terms with the higher powers of t are usually less significant and the point of diminishing returns is reached with the second integration.

Furthermore, third order systems are typically less stable. The significance of each term in both acquisition and dynamic tracking capabilities is readily appreciated by considering the analogous situation with the phase-locked loop. Thus $T_i(o)$ corresponds to an initial phase offset which is readily acquired. αt corresponds to a phase rate of change or frequency offset. A small frequency offset is readily acquired, but for large offsets the acquisition time grows exponentially until a point is reached where acquisition is no longer possible. The term $\beta(t^2/2)$ represents a rate of change of frequency. This term by itself presents no acquisition problem, but if the term αt is also present, then this term aids or hinders acquisition depending on whether it acts to decrease or increase the frequency offset. (Ref.14) The term $\gamma(t^3/6)$ is frequently an impulse in practical situations where it drops to zero before there has been any significant phase change on the input signal. β and γ result in significant dynamic tracking errors only after they have been non zero for a substantial period of time. As a practical matter this situation is, in general, fairly easy to cope with, especially with γ. In those situations where $\beta(t^2/2)$ becomes excessive, a double integration is required. It should also be noted that the acquisition procedure with a split gate tracker is more complex than that of the phase-locked loop because of the necessity to search for the incoming pulse. In this respect α and β represent even stronger constraints on the acquisition capability.

Comparison With Other Systems

In this section the split gate tracker is compared with two other range measurement systems, the leading edge tracker, and the harmonic ranger.

Leading error detection -- The leading edge tracker differs from the split gate tracker in that its gate is designed to detect and follow the leading edge of the signal pulse rather than the center of gravity. Since this type of system utilizes a relatively small portion of the signal energy, a higher signal-to-noise ratio is required. The advantage of the leading edge tracker is its specialized range resolution capability. Thus, in a situation with many closely spaced echos, it is able to track the earliest echo even if there is a substantial overlapping among the echos.

The analysis of the leading edge tracker follows that of the split gate tracker. Both systems function as tracking filters and have the same type of dynamic response. The IF amplifier preceding the leading edge tracking loop is much wider than that considered earlier for the split gate loop in order to retain the fast rise time of the signal pulse. However the same baseband representation of the IF amplifier, a double RC rolloff, may be employed.

A picture of the gate and its relationship to the leading edge is shown in Figure C-12. The filtering preceding the loop is the same as that of Figure C-6 with the understanding that the corner frequency a has been increased. The transform representation is the same as that shown in Figure C-5. The amplitude of the signal pulse applied to the lowpass signal is given, as before, by V_o. The filtered pulse of Figure C-12 reaches this value after the transient has died out.

The first step in the analysis is to compute the mean square value of the noise voltage in terms of the autocorrelation functions as is indicated by Eq. (C-9). $R_m(\tau)$ is given, as before, by Eq. (C-12). $R_g(\tau)$ may be found by inspection with the aid of Figure C-13 in which the gate has unity amplitude and a width τ_g. The value of the noise voltage given by Eq. (C-9) may now be expressed directly in terms of the system parameters for $R_m(\tau)$ and $R_g(\tau)$. Thus,

$$\overline{e_n^2} = (2)\left(\frac{N_o a}{4}\right)\cdot \int_o^{\tau_g} (1+a\tau)e^{-a\tau}(-\tau+\tau_g)\, d\tau \qquad \text{(C-39)}$$

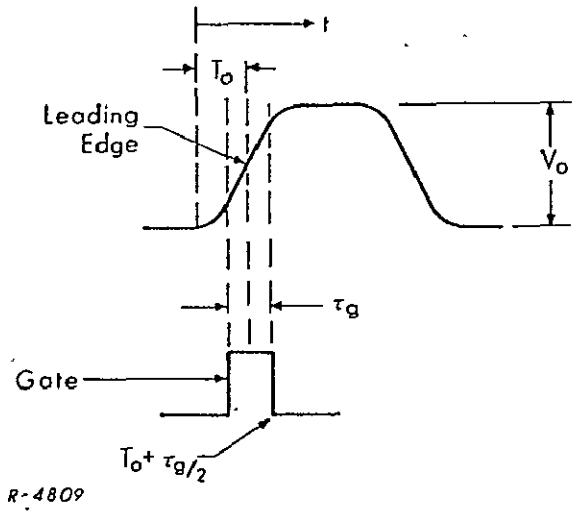

Figure C-12 Leading Edge Gate

Evaluating the integral gives

$$\overline{e_n^2} = \frac{N_o}{2}\left[2\tau_g - \frac{3}{a} + \frac{3}{a}e^{-a\tau_g} + \tau_g e^{-a\tau_g}\right] = \frac{N_o \tau_g}{2} f_3(a\tau_g) \qquad \text{(C-40)}$$

where the function $f_3(a_1\tau_g)$, plotted in Figure C-14, has been introduced to simplify the notation.

The next step is to compute the error voltage produced by the gate as a function of its position relative to the leading edge of the pulse. This requires a description of the leading edge in terms of the pulse parameters and the filtering which shape the leading edge.

It is clear that the shape of the pulse depends on its duration and on the bandpass characteristic of the filter. Thus if the input to the filter is a rectangular pulse of long duration, the output of the filter is a pulse of the same amplitude V_o and has leading and trailing edges described by the expression of Eq. (C-16). If the input pulse is of short duration, the output pulse fails to reach the amplitude V_o as was seen in the earlier example depicted in Figure C-9. A more general description of the leading edge is presented in Figure C-15 which contains a plot of Eq. (C-16) for several values of the parameter $a\tau_p$.

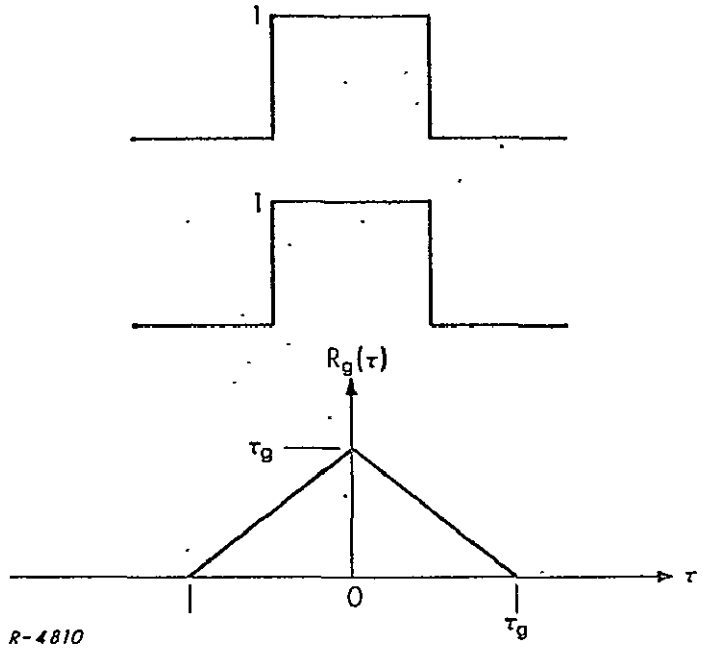

Figure C-13 $R_g(\tau)$ for Leading Edge Tracker

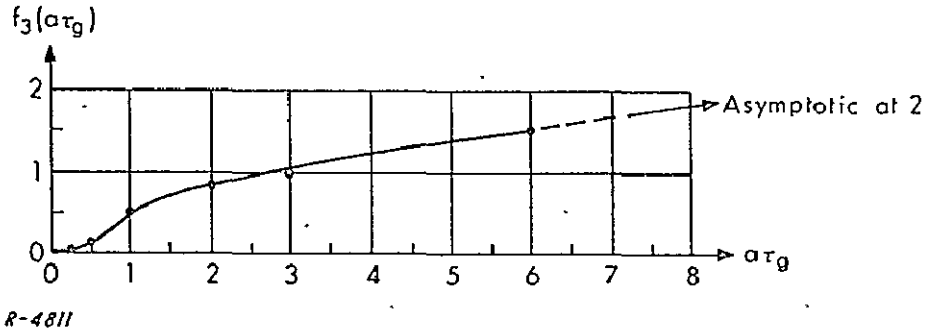

Figure C-14 Plot of $f_3(a\tau_g)$

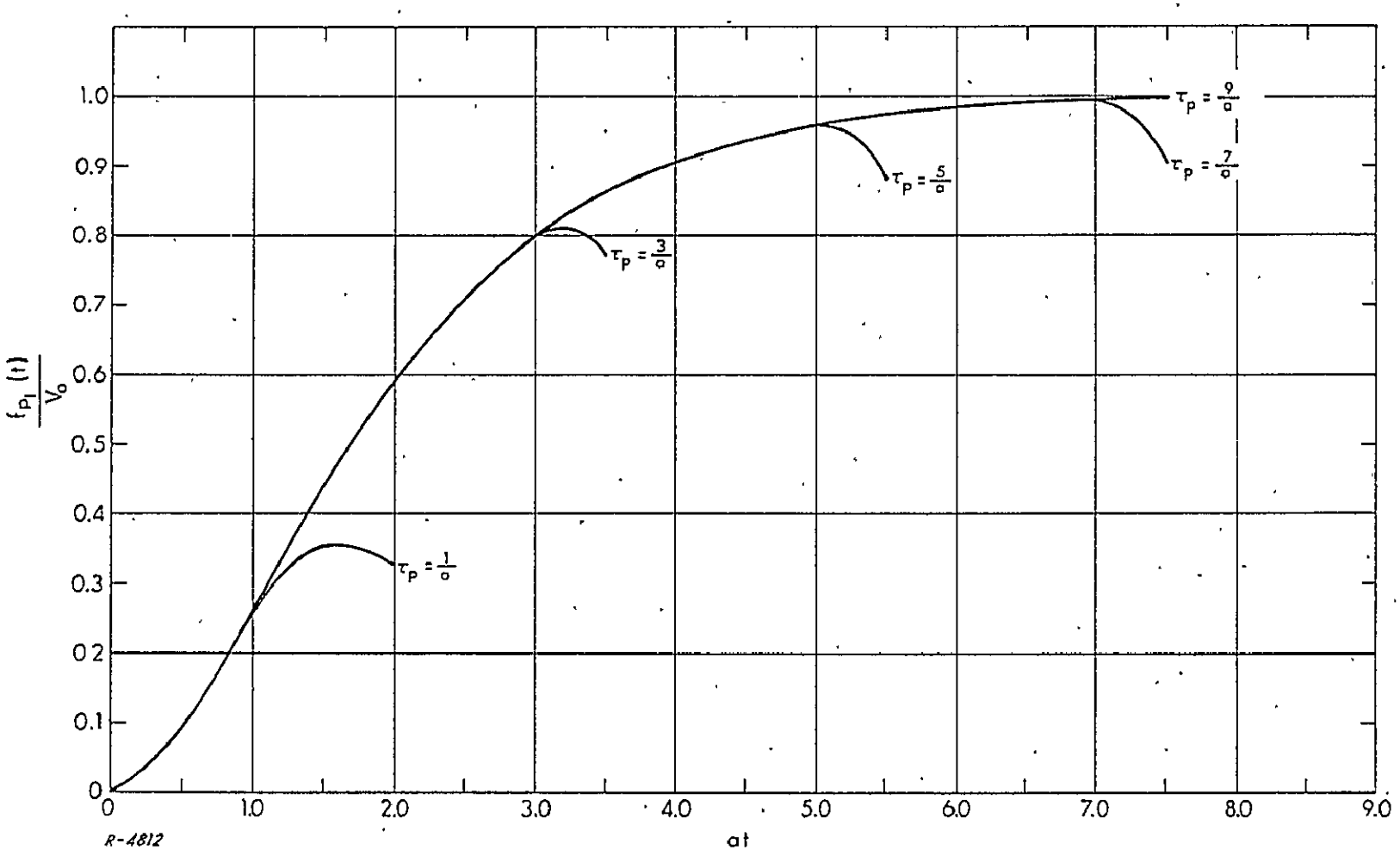

Figure C-15 Leading Edge Versus Pulse Duration

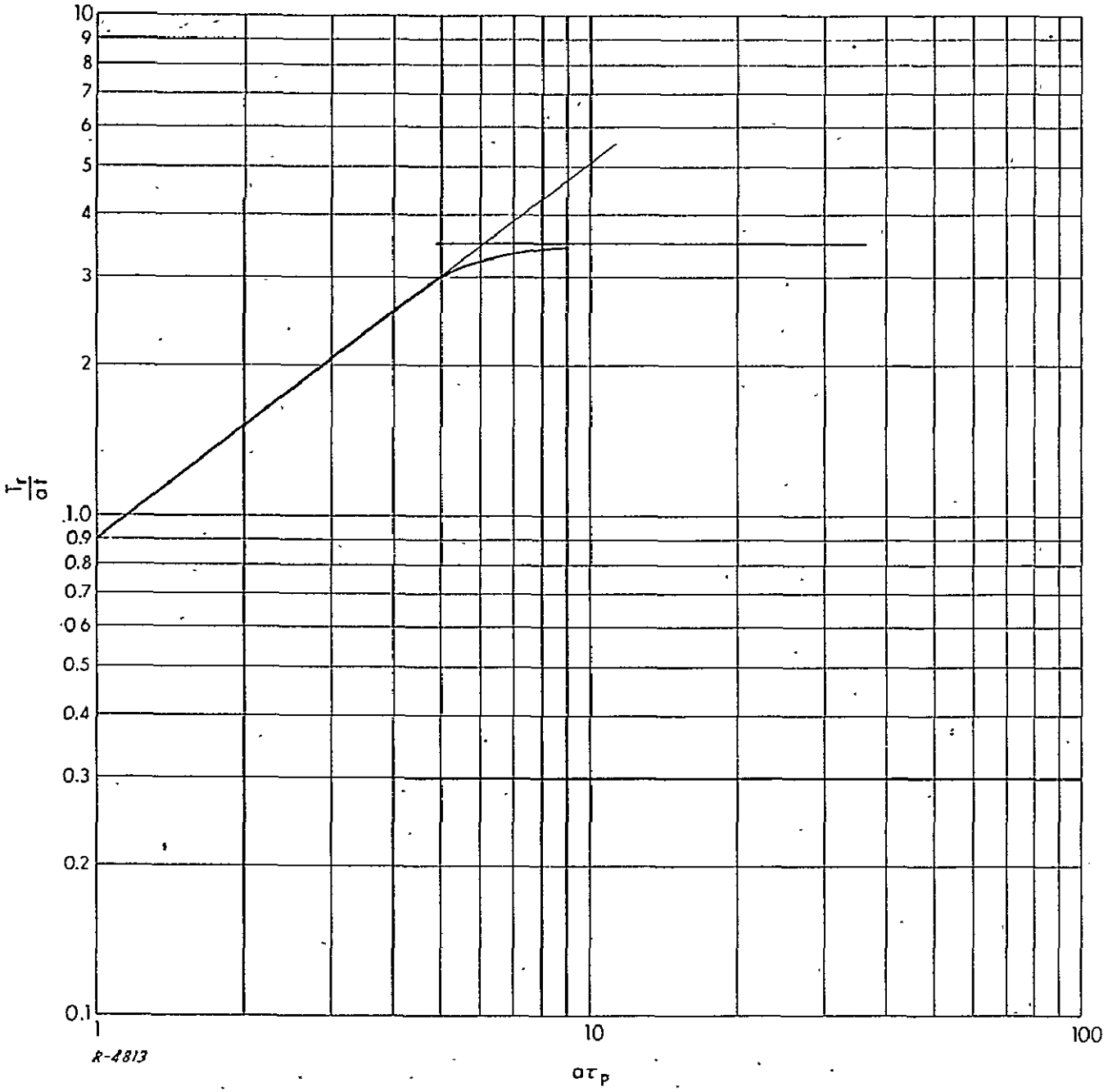

Figure C-16 Rise Time Versus Pulse Duration

The peak value of the pulse varies rapidly for small values of $a\tau_p$ and asymptotically reaches the maximum value as $a\tau_p$ becomes large. The major concern here is the form of the leading edge and its dependence on $a\tau_p$. In a typical leading edge tracking system the IF bandwidth is large enough to preserve a fast rise time. This is equivalent to a large value of $a\tau_p$. It is apparent from the figure that $a\tau_p \approx 6$ is a sufficiently large value such that further increases in the pulse duration do not have more than a negligible effect on the leading edge.

The value $a\tau_p \approx 6$ may be determined more precisely by plotting the pulse rise time for each of the pulses shown in Figure C-15 . The rise time T_r is defined as the time required for the pulse amplitude to rise from 10% to 90% of its peak value. A plot of (T_r/at) versus $a\tau_p$ is shown in Figure C-16. The breakpoint at $a\tau_p \approx 6$ is indicated by the intersection of the asymptotes to the curve.

The error voltage produced by the gate depends on the gate width and the location of the center of the gate relative to the leading edge. In view of the lack of symmetry in the leading edge it is clear that the optimum value of the gate width τ_g depends on the location of the center of the gate. To simplify the situation, the leading edge curve for $a\tau_p>6$ is approximated by $\sin^2(\pi at/8)$. This approximation provides symmetry about the midpoint of the leading edge and is independent of τ_p for all $a\tau_p>6$.

The error voltage e_e is given by the area under the curve of the leading edge falling within the gate, minus a reference voltage. Thus

$$e_e = \int_{T_o-\tau_g/2+\Delta t}^{T_o+\tau_g/2+\Delta t} V_o \sin^2(\pi at/8)\,dt - \int_{T_o-\tau_g/2}^{T_o+\tau_g/2} V_o \sin^2(\pi at/8)\,dt \quad (C-41)$$

where the second integral is the reference voltage and $T_o + \Delta t$ is the location of the center of the gate. The term Δt is the timing error in the gate position.

Evaluating the integrals gives

$$e_e \cong V_o \Delta t \sin(\pi a \tau_g/8) \sin(\pi a T_o/4) \quad (C-42)$$

where the small angle approximation $\sin(\pi a\Delta t/4) \approx \pi a\Delta t/4$ has been made.

The gate width which results in a minimum value of Δt due to noise perturbations is found by equating e_e given by Eq. (C-42) with e_n given by Eq. (C-40). The equation is then solved for Δt giving an expression which has a minimum value for the appropriate selection of the parameter $a\tau_g$. Equating e_e with e_n gives

$$V_o \Delta t \sin(\pi a \tau_g / 8) \sin(\pi a T_o / 4) = \sqrt{(N_o/2)\, \tau_g f_3(a\tau_g)} \qquad \text{(C-43)}$$

At this point T_o may be set for the midpoint of the leading edge, that is for $(\pi a\, T_o/8) = \pi/4$ radians, so that $aT_o = 2$. The timing error Δt is replaced by σ_t to indicate the rms value. Then solving for σ_t gives

$$\sigma_t = \frac{N_o}{\sqrt{2aV_o^2}} \left(\frac{\left[2a\tau_g - 3(1-e^{-a\tau_g}) + a\tau_g e^{-a\tau_g}\right]^{1/2}}{\sin(\pi a \tau_g / 8)} \right) \qquad \text{(C-44)}$$

The function of $a\tau_g$ enclosed by the brackets has a minimum value of 1.79 at $a\tau_g \approx 1$ as shown by the graph of this function in Figure C-17. The value of $a\tau_g$ is not critical as may be seen from the relatively flat curve in the vicinity of the minimum. Substituting the minimum value gives

$$\sigma_{t_{min}} = 1.26 \sqrt{\frac{N_o}{aV_o^2}} \qquad \text{(C-45)}$$

The rms timing error σ_t can be expressed in terms of the pulse energy $E_o = (V_o^2/2)\tau_p$ by substituting for V_o. Thus

$$\sigma_{t_{min}} = 1.26 \sqrt{\frac{N_o \tau_p}{aE_o}} \qquad \text{(C-46)}$$

The derivation of σ_t has assumed any value of τ_p for $a\tau_p \geq 6$. As a practical matter it is desireable to conserve signal energy by avoiding the use of a pulse width of unnecessarily long duration. Hence, set $\tau_p = 6/a$. Substituting this value for τ_p into Eq. (C-46) gives

$$\sigma_{t_{min}} = \frac{3.1}{a\sqrt{R}} \qquad \text{(C-47)}$$

where $R = 2E_o/N_o$.

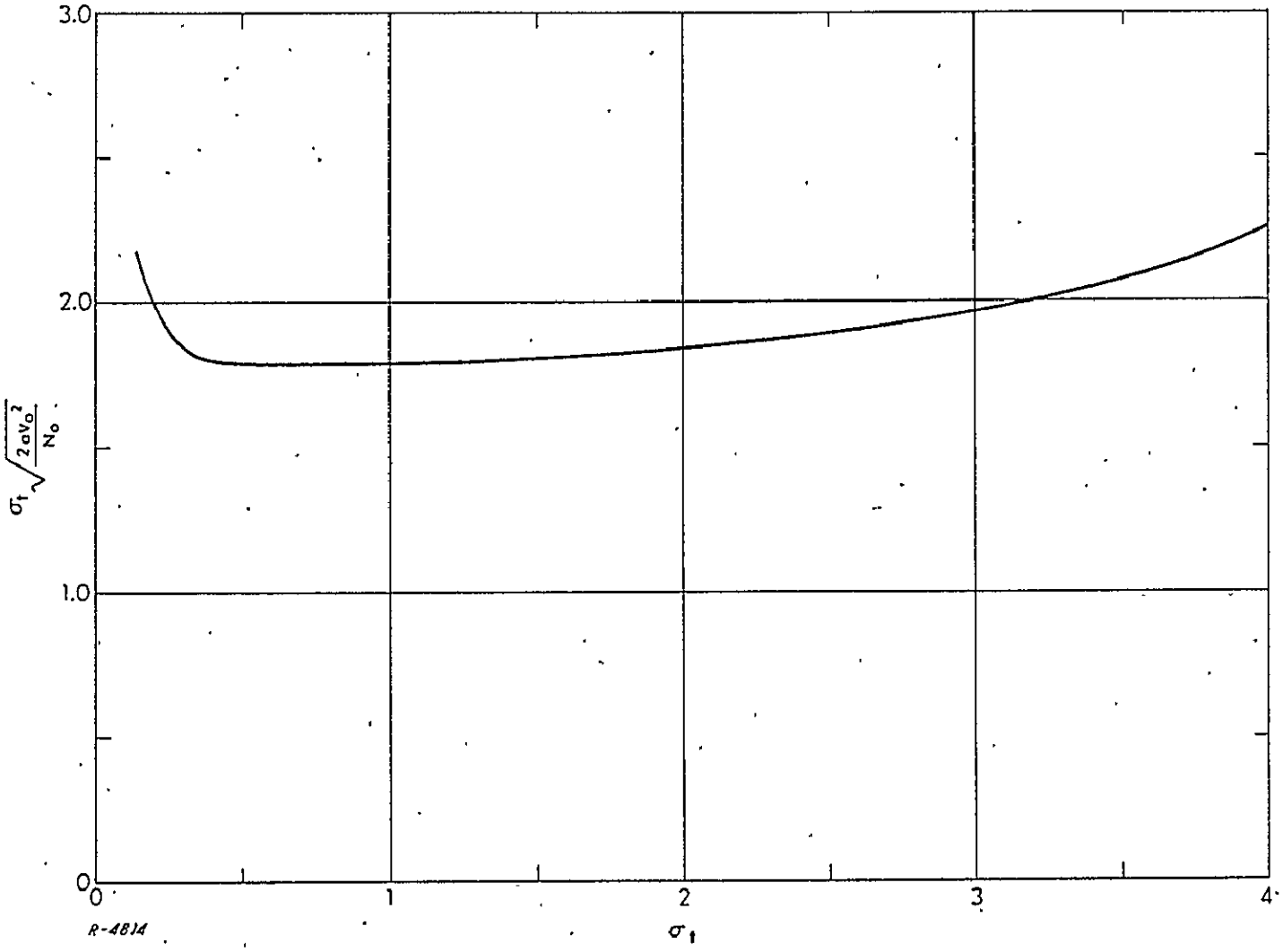

Figure C-17 Minimization of σ_t

It is interesting to compare the minimum values of σ_t for the split gate and leading edge trackers as given by equations (C-26) and (C-47). On an energy basis, the split gate tracker is superior.

The effect of the tracking filter following the gate is identical to that of the split gate tracking loop so that σ_t for the complete system is given by

$$\sigma_{t_{min}} = \frac{3.1}{a\sqrt{\frac{Save}{N_o B_n}}} \qquad \text{(C-48)}$$

Harmonic tone ranging systems. -- Tone ranging systems extract range data from the phase differences between a continuing form of the transmitted pure tone and the received tone that has been delayed by the two-way transmission over the channel between the target and the ground station.

A series of tones of ascending frequency are generally employed to resolve the ambiguity inherent in the modulo 2π phase of a pure sinusoid. This gives rise to the name "harmonic tone ranging systems", although the relationship of the tone frequencies is not required to be precisely harmonic.

The 2π ambiguity of the highest, or finest, tone is resolved by the phase shift measured on the next lowest tone, whose ambiguity is in turn resolved by the phase of the next lowest tone and so on. The effect of this is to establish a non-modulo 2π phase detection system, i. e, a detector that responds linearly to phase shifts exceeding 2π radians with no discontinuities or bounds in its characteristic. Usually the lower tones are synthesized coherently from the directly generated highest range tone so that the errors in the extraction of phase information from the highest tone set the limitations on the fundamental accuracy.

Ambiguity resolution. -- Ambiguity resolution can be accomplished when a number of tones are transmitted, one of which is used for ranging and the rest for ambiguity resolution. In principle, once the target is acquired, there is no further need to transmit the ambiguity resolving tones. Thus, the accuracy can be increased by diverting signal power to the retained tone. Of course, such accuracy improvement is obtained by trading off all of the system's ambiguity resolving capability.

As an example, consider a system in which the power in the ambiguity resolving side tones is reduced relative to the power in the ranging tone. The ranging accuracy is enhanced while ambiguity performance is reduced somewhat, but not below the point where the ambiguity resolving system is effective. If the system under consideration has four ranging tones with frequencies related in a 16:1 ratio, the accuracy, in phase, required in each of the ambiguity resolving tones is roughly $360/32 = 11.1$ degrees for marginal ambiguity resolution performance. On the other hand, the accuracy, in phase, required for the highest ranging tone is usually a fraction of a degree (consider, for example, the case where the highest ranging tone is 1mc and the range accuracy required is 1 ft). With the help of Eq. (B-13) it can be seen that the power in each of the ambiguity resolving tones can be reduced considerably relative to the power in the highest ranging tone. The Goddard Range and Range Rate system is a harmonic ranging system design which is based on this technique.

Another practical technique that yields similar results (namely, increased accuracy at the expense of reduced ambiguity resolution performance) is designed into the WSMR DME system. In this system, the four tones VF (very fine), F (fine), C (coarse) and VC (very coarse) are combined to form a new set of tones closely spaced about the highest ranging tone, VF. The new frequencies are VF-F, VF-(C+VC), VF, and VF + C. Each of these tones is treated as if it were the highest ranging tone. The range measurements derived from the four tones are averaged, hence the over-all rms accuracy is doubled. However, since recovery of the phases of the original ambiguity resolving tones involves linear combining of at least two of the new tones, the errors in each of the reconstituted ambiguity resolving tones is increased by at least a factor of $\sqrt{2}$. Note that in the arrangement indicated above recovery of two of the ambiguity resolving tones is possible by operations on two tones at a time. Thus, the increase in error is just $\sqrt{2}$. In any case, the error in a rederived ambiguity resolving tone is proportional to the square root of the number of received tones used to derive it and since the accuracy requirement on fine range tones is high, reliable ambiguity resolution is assured.

In summary, there are several techniques that can be used to improve the accuracy obtainable with the range tone system. The techniques involve careful modification of the ambiguity resolving tones and result in improved accuracy with some allowable degradation in ambiguity resolution performance.

Fundamental detection systems. -- There are two basic approaches to the extraction of range information in tone ranging systems, which differ in the manner of realization of the non-modulo 2π detector. These are phase detection and time measurement detection.

The ideal channel (including the target) over which the range tones are transmitted can be characterized as a pure delay by

$$C(s) = e^{-\tau s} \tag{C-49}$$

where τ is the two-way transit time. The effect of this channel upon a pure sinusoid is to introduce a phase delay linearly related to τ. Two detection schemes are thus indicated; in one the actual phase difference between transmitted and received highest range tone is measured and then converted to range, in the other the actual time delay τ is measured and then converted to range.

Phase measurement. -- A basic model of a phase measuring system is shown in Figure C-18. Let

$$v_r(t) = a_r(t) \cos \theta_r(t) \tag{C-50}$$

Then

$$v_r(t-\tau) = a_r(t-\tau) \cos \theta_r(t-\tau) \tag{C-51}$$

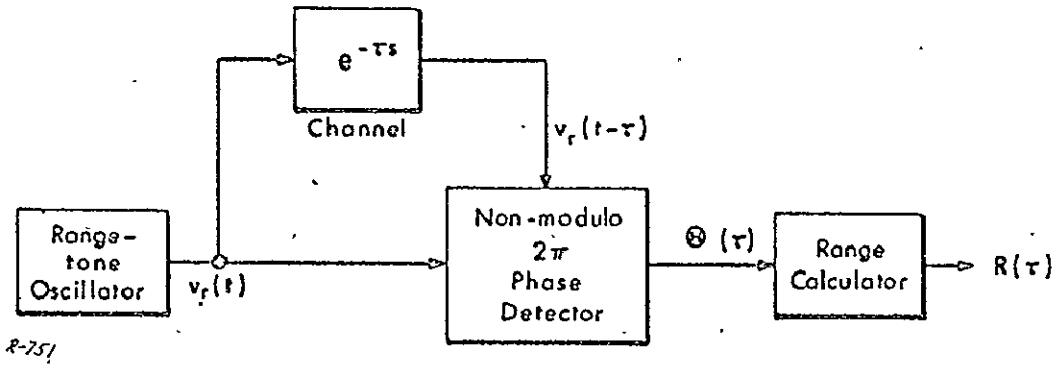

Figure C-18 Phase Measuring System

The phase detector forms

$$\theta(\tau) = \theta_r(t) - \theta_r(t-\tau) \tag{C-52}$$

Equation (C-52) can be written as

$$\theta(\tau) = \int_{t-\tau}^{t} \dot{\theta}_r(\mu)\, d\mu \tag{C-53}$$

For a perfectly stable and undisturbed ranging tone

$$\theta_r(t) = 2\pi f_r t, \tag{C-54}$$

where f_r is the frequency of the tone in Hz. Substitution in Eq. (C-52) yields

$$\theta(\tau) = 2\pi f_r \tau \tag{C-55}$$

Now the range of the target, defined as $r(\tau)$, is related to τ by

$$r(\tau) = \frac{c\tau}{2} \tag{C-56}$$

where c is the propagation velocity in the intermediate channel. Thus

$$r(\tau) = \frac{c}{4\pi f_r} \cdot \theta(\tau). \tag{C-57}$$

Time measurement. -- A basic model of a time measuring system is shown in Figure C-19.

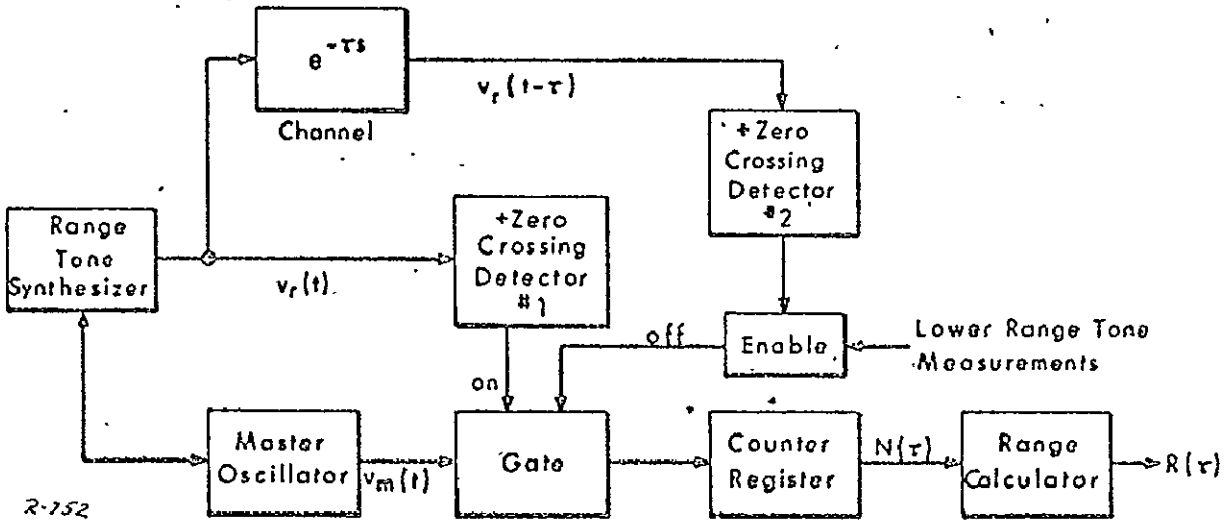

Figure C-19 Time Measurement System

Figure C-20 shows the operation of the system in detail. The counter is gated on at time t_o by a positive-going zero crossing of $v_r(t)$, as sensed by zero crossing detector No. 1. Detector No. 2 sends gate-off pulses at every positive-going zero-crossing of $v_r(t-\tau)$. The phase or time information obtained from the lower range-tones determines how many of these off pulses should be blocked to remove the cycle ambiguity in $v_r(t-\tau)$. Thus the proper pulse is passed; terminating the master oscillator signal input to the counter accumulating register. The counter reads $N(\tau)$ where N is the total number of periods of the master oscillator signal that have occurred during the time τ. Let the master oscillator signal be

$$v_m(t) = a_m \cos \theta_m(t) \tag{C-58}$$

For a perfect oscillator of frequency f_m Hz,

$$\theta_m(t) = 2\pi f_m t \tag{C-59}$$

The value of f_m is chosen very large with respect to f_r so that errors in counting f_m amounting to less than one whole cycle would be negligible. Thus, for computation of range, $N(\tau)$ is related to τ by

$$N(\tau) = f_m \tau \tag{C-60}$$

so that

$$r(\tau) = \frac{c}{2f_m} \cdot N(\tau) \tag{C-61}$$

Target dynamic accuracy limitations. -- Let us consider how doppler shift and doppler rate influence the range error as a function of f_m and f_r. Differentiating Eq. (C-57) and Eq. (C-61) twice with respect to time, we obtain

$$\dot{r}(\tau) = \frac{c}{4\pi f_r} \dot{\theta}(\tau) \tag{C-62}$$

$$\ddot{r}(\tau) = \frac{c}{4\pi f_r} \ddot{\theta}(\tau) \tag{C-63}$$

$$\dot{r}(\tau) = \frac{c}{2f_m} \dot{N}(\tau) \tag{C-64}$$

$$\ddot{r}(\tau) = \frac{c}{2f_m} \ddot{N}(\tau) \tag{C-65}$$

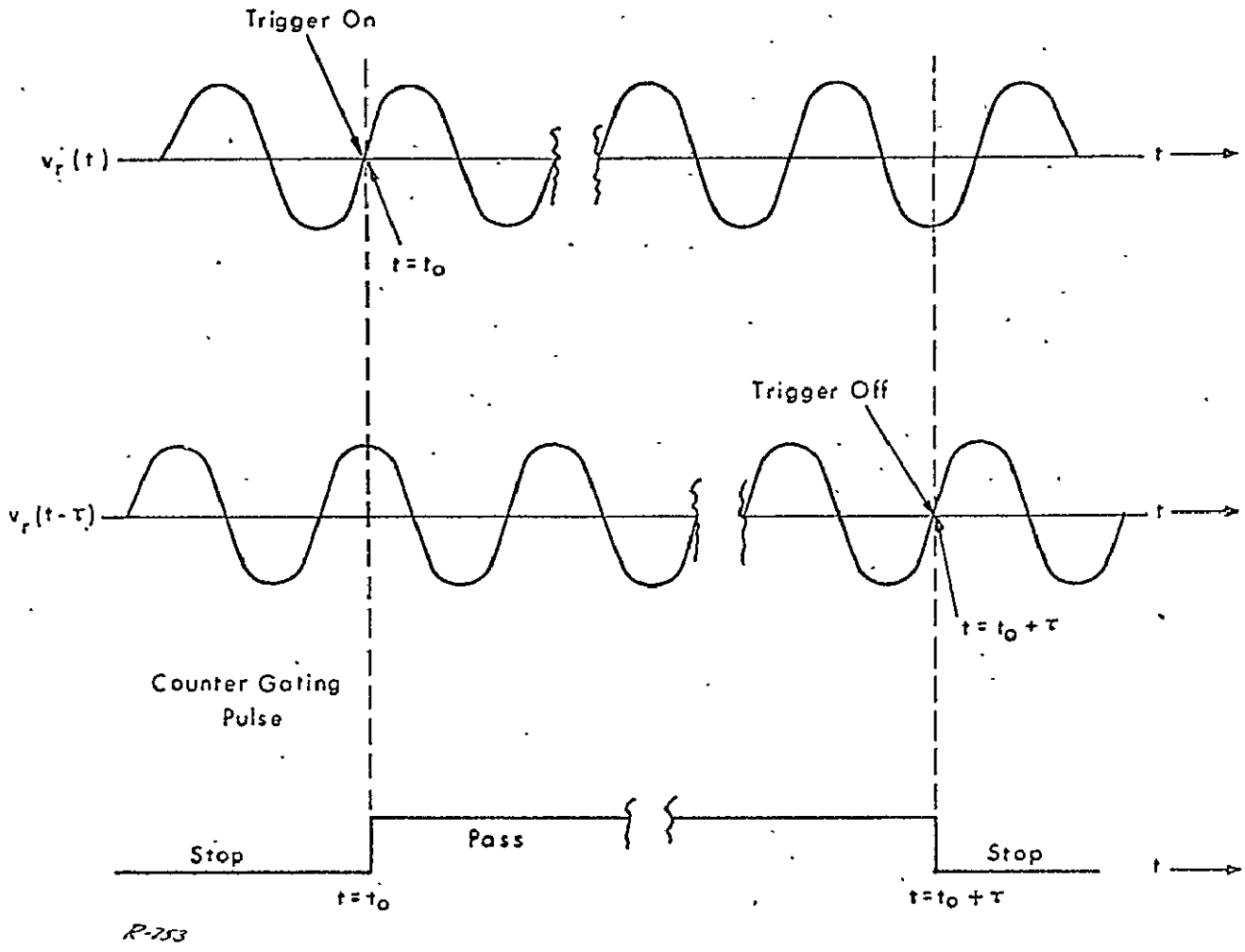

Figure C-20. Time Detection Process

Equations (C-62) through (C-65) are linear relationships. Thus for a given post-detection filtering characteristic in both systems, the error in the detected quantity, either $\theta(\tau)$ or $N(\tau)$, varies linearly with f_m or f_r, for a given range rate and acceleration. However, the conversion of the detected quantity to range information inverts the linear relationships, so that the range error caused by post-detection filtering in the presence of target dynamics is independent of f_m and f_r.

The same argument may be offered for predetection filtering with the exception that such filters may be required to track doppler-shifted signals, and thus have limited phase (or frequency) error dynamic ranges, before unlocking or else excessive attenuation results. Hence the actual phase error must be considered at some point to ensure that IF filters and/or phase-locked loops will be operated within their appropriate offset limits. The amount of $\dot{\theta}(\tau)$ or $\ddot{\theta}(\tau)$ corresponding to a given $\dot{r}(\tau)$ or $\ddot{r}(\tau)$ is, of course, directly proportional to f_r as shown by Eqs. (C-57), (C-62), and (C-63). Thus there may be some upper limit on f_r set by tracking limitations of PLL or bandwidth limitations of IF filters.

When a PLL is utilized as the tracking filter the dynamic tracking errors are the same as those given for the PLL of Appendix B. In more complex systems where a carrier derived rate aiding signal is provided the dynamic error may be substantially reduced without any increase in the PLL bandwidth. However in such a system the PLL bandwidth would be reduced somewhat to provide an improvement in both the dynamic and the noise errors.

Noise limitations. -- Consider the phase detecting system in which the detector is followed by a filter whose noise bandwidth is B_n Hz, where B_n is defined by Eq. (B-14) above. Now

$$\overline{\theta_n^2} = \frac{1}{2(S/N)_{B_n}} \qquad \text{(C-66)}$$

where $\overline{\theta_n^2}$ is the mean square detected and filtered output caused by additive noise in the received signal, and $(S/N)_{B_n}$ is the ratio of signal power to noise power passed by the filter. By Eq. (C-57)),

$$\Delta r(\text{rms}) = \frac{c}{4\pi f_r} \cdot \frac{1}{\sqrt{2(S/N)_{B_n}}} \qquad \text{(C-67)}$$

where $\Delta r(\text{rms})$ is an rms range error caused by noise.

In the case of the time measurement system, the error in time τ is related to the phase error by Eq. (C-55). Consequently,

$$\Delta\tau(\text{rms}) = \frac{1}{2\pi f_r \sqrt{2(S/N)_{B_n}}} \tag{C-68}$$

where we have assumed that the output $N(\tau)$ is operated upon by a filter with noise bandwidth B_n. The resulting rms error in range measurement is

$$\Delta r(\text{rms}) = \frac{c}{4\pi f_r} \cdot \frac{1}{\sqrt{2(S/N)_{B_n}}} \tag{C-69}$$

which is seen to be identical to Eq. (C-67).

If the ranging measurement is based on two range tones which are combined in the signal spectrum so that both lines fall near the edge of the signal bandwidth, then the range error given by Eq. (C-69) is reduced by a factor of $\sqrt{2}$. Similarly, if three such tones are utilized the range error is reduced by $\sqrt{3}$.

The preceding formulations are based on the power of the ranging tone. These formulations may also be expressed in terms of the total transmitted signal power S_T. Thus, for example, if the transmitted signal e(t) is in the form of a PM/ PM waveform, namely

$$e(t) = A \cos\left[\omega_c t + \delta_{sc} \sin(\omega_{sc} t + \sum_{j=1}^{k} \delta_{ssj} \sin \omega_{ssj} t)\right] \tag{C-70}$$

Where the subscript sc designates a subcarrier and the subscript ss designates a sub-sub-carrier. The summation indicates that there may be a number of sub-sub-carriers, i.e., k sub-sub-carriers. The amplitudes of the various carriers are proportional to the modulation indexes, and their powers are proportional to the squares of the modulation indexes for $\delta \ll 1$. The expression for the phase error of Eq. (C-66) may be expressed in terms of the total signal power S_T by

$$\Delta\phi_{sc}(\text{rms}) \approx \frac{1}{\delta_{sc}} \left(\frac{S_T}{N}\right)^{-1/2}_{B_n} \tag{C-71}$$

for a measurement of the subcarrier and by

$$\Delta\phi_{ssj}(\text{rms}) \approx \frac{1}{\delta_{sc}\delta_{ssj}} \left(\frac{S_T}{2N}\right)^{-1/2}_{B_n}$$

for a measurement of j^{th} sub-sub-carrier. Note that the factors of 2 appearing in these expressions arise because the average power in a sinusoid of amplitude δ is equal to $\delta^2/2$. The result is easily derived when it is recognized that demodulation of the PM subcarrier (or sub-sub-carriers) results in coherent addition of its upper and lower sideband while the noise components in the vicinity of the sidebands are added incoherently.

REFERENCES

1. Siebert, W. M., "A Radar Detection Philosophy," IRE Trans. on Information Theory Symposium, IT-2, 204, 1954.

2. Peterson, W. W., Birdsol, T. G. and Fox, W. C., "The Theory of Signal Detectability," IRE Trans. on Information Theory, PGIT-4, 171, 1954.

3. Woodward, P. M., Probability and Information Theory with Applications to Radar, Pergamon Press, New York, 1953.

4. Gabor, D., "Theory of Communication," Journal IEE, 93, 111, 429, 1946.

5. Davenport, W. B. and Root, W. L., An Introduction to the Theory of Random Signals and Noise, McGraw-Hill, New York, 1958.

6. Manasse, R., "Range and Velocity Accuracy from Radar Measurements," Lincoln Lab. Group Report, 312-26, 1955.

7. Mallinkrodt, A. J., "Passive Ranging Doppler System," Report No. 961-R1, Nov. 1953, Contract DA-04-495-ORD-483, Ballistic Research Labs., Aberdeen, Maryland.

8. ADCOM, Inc., "Performance of the AROD Tracking System," Seventh Progress Report, Contract No. NAS8-2675, Nov. 1963.

9. Davenport, Jr., W. B., "Signal-to-Noise Ratios in Bandpass Limiters," Journal of Applied Physics, Vol. 24, No. 6, pp. 720-27, June 1953.

10. "Study, Evaluation and Analysis of Unified S-Band System for Apollo Ground Network," ADCOM, Inc., Cambridge, Mass., Sept. 1964.

11. Mallinkrodt, A. J. and Sollenberger, T. E., "Optimum Pulse Time Determination," IEEE Trans. on Information Theory, Vol. IT-3, pp. 151-59, March 1954.

12. Skolnik, M. I., Introduction to Radar System, McGraw-Hill, New York 1962.

13. Barton, D. K., Radar Systems Analysis, Prentice Hall, New Jersey, 1964.

14. "The Design of a WSMR Electronic Trajectory Measurement Facility," ADCOM, Inc., Cambridge, Mass., 1967, Chap. 2.